การเตรียม ZSM-5 บนเส้นใยอิเล็กโทรสปันซิลิกาสำหรับคาร์บอนมอนอกไซด์ไฮโดรจิเนชัน

นางสาวกิติยา เลิศสกุลบรรลือ

วิทยานิพนธ์นี้เป็นส่วนหนึ่งของการศึกษาตามหลักสูตรปริญญาวิทยาศาสตรมหาบัณฑิต
สาขาวิชาปิโตรเคมีและวิทยาศาสตร์พอลิเมอร์
คณะวิทยาศาสตร์ จุฬาลงกรณ์มหาวิทยาลัย
ปีการศึกษา 2556

PREPARATION OF ZSM-5 ON ELECTROSPUN SILICA FIBER FOR CARBON MONOXIDE HYDROGENATION

Miss Kitiya Lertskulbanlue

A Thesis Submitted in Partial Fulfillment of the Requirements
for the Degree of Master of Science Program in Petrochemistry and Polymer Science
Faculty of Science
Chulalongkorn University
Academic Year 2013

Thesis Title	PREPARATION OF ZSM-5 ON ELECTROSPUN SILICA FIBER FOR CARBON MONOXIDE HYDROGENATION
By	Miss Kitiya Lertskulbanlue
Field of Study	Petrochemistry and Polymer Science
Thesis Advisor	Assistant Professor Prasert Reubroycharoen, D.Eng.

Accepted by the Faculty of Science, Chulalongkorn University in Partial Fulfillment of the Requirements for the Master's Degree

.....Dean of the Faculty of Science

(Professor Supot Hannongbua, Dr.rer.nat.)

THESIS COMMITTEE

.....Chairman

(Professor Pattarapan Prasassarakich, Ph.D.)

.....Thesis Advisor

(Assistant Professor Prasert Reubroycharoen, D.Eng.)

.....Examiner

(Associate Professor Wimonrat Trakarnpruk, Ph.D.)

.....External Examiner

(Assistant Professor Chanatip Samart, D.Eng.)

กิติยา เลิศสกุลบรรลือ : การเตรียม ZSM-5 บนเส้นใยอิเล็กโทรสปันซิลิกาสำหรับคาร์บอนมอนอกไซด์ไฮโดรจิเนชัน. (PREPARATION OF ZSM-5 ON ELECTROSPUN SILICA FIBER FOR CARBON MONOXIDE HYDROGENATION) อ.ที่ปรึกษาวิทยานิพนธ์หลัก: ผศ. ดร. ประเสริฐ เรียบร้อยเจริญ , 79 หน้า.

การสังเคราะห์ ZSM-5 บนเส้นใยอิเล็กโทรสปันซิลิกาสำหรับปฏิกิริยาคาร์บอนมอนอกไซด์ไฮโดรจิเนชัน (CO hydrogenation reaction) ถูกเตรียมโดยกระบวนการไฮโดรเทอร์มอล และพิสูจน์เอกลักษณ์ด้วยเทคนิค XRD, SEM, EDX, BET และ TPR ปัจจัยที่มีผลต่อการยึดเกาะของ ZSM-5 บนเส้นใยอิเล็กโทรสปันซิลิกาได้รับการศึกษาโดยการแปรผันของพีเอชในสารละลาย (8-10) เวลาไฮโดรเทอร์มอล (24-72 ชั่วโมง) อุณหภูมิไฮโดรเทอร์มอล (170-190 องศาเซลเซียส) และสัดส่วนซิลิกอนต่ออะลูมิเนียม (20-80) จากผลการทดลองพบว่าภาวะที่เหมาะสมต่อการเตรียม ZSM-5 บนเส้นใยอิเล็กโทรสปันซิลิกา คือ พีเอช 9 ด้วยภาวะไฮโดรเทอร์มอล 180 องศาเซลเซียส เป็นเวลา 24 ชั่วโมง การเพิ่มสัดส่วนซิลิกอนต่ออะลูมิเนียมจาก 20 เป็น 80 ส่งผลให้ ZSM-5 ยึดเกาะบนเส้นใยเพิ่มขึ้น สมบัติการเร่งปฏิกิริยาของเส้นใยอิเล็กโทรสปันซิลิกา ZSM-5 บนเส้นใยอิเล็กโทรสปันซิลิกา (สัดส่วนซิลิกอนต่ออะลูมิเนียม 20-80) ซิลิกาอุตสาหกรรม (แบบรูพรุน) และ ZSM-5 อุตสาหกรรม (แบบรูพรุน) ที่มีโคบอลต์ร้อยละ 10 โดยน้ำหนัก ได้รับการศึกษาโดยใช้ปฏิกิริยาคาร์บอนมอนอกไซด์ไฮโดรจิเนชัน ที่มีสัดส่วนไฮโดรเจนต่อคาร์บอนมอนอกไซด์ 2:1 อัตราการไหลของแก๊ส 75 มิลลิลิตร/นาที/กรัม และอุณหภูมิในการเกิดปฏิกิริยา 280 องศาเซลเซียส ผลการทดลองแสดงว่า การเพิ่มสัดส่วนซิลิกอนต่ออะลูมิเนียมจาก 20 เป็น 80 ส่งผลให้ค่าร้อยละการเปลี่ยนคาร์บอนมอนอกไซด์เพิ่มขึ้นจากร้อยละ 34.29 เป็น 42.99 ในขณะค่าความจำเพาะต่อการเกิดมีเทนมีแนวโน้มลดลงจาก 93.10 เป็น 88.33 ZSM-5 ที่สังเคราะห์บนเส้นใยอิเล็กโทรสปันซิลิกาที่มีสัดส่วนซิลิกอนต่ออะลูมิเนียม 80 ให้ค่าการเปลี่ยนคาร์บอนมอนอกไซด์สูงสุด (ร้อยละ 42.99) และที่สัดส่วนซิลิกอนต่ออะลูมิเนียม 20 ให้ค่าความจำเพาะต่อการเกิดมีเทนสูงสุด (ร้อยละ 93.10)

สาขาวิชา ปิโตรเคมีและวิทยาศาสตร์พอลิเมอร์ ลายมือชื่อนิสิต .....

ปีการศึกษา 2556 ลายมือชื่อ อ.ที่ปรึกษาวิทยานิพนธ์หลัก .....

5472228423 : MAJOR PETROCHEMISTRY AND POLYMER SCIENCE
KEYWORDS: ZSM-5 / HYDROTHERMAL / ELECTROSPUN SILICA FIBERS / CO HYDROGENATION

KITIYA LERTSKULBANLUE: PREPARATION OF ZSM-5 ON ELECTROSPUN SILICA FIBER FOR CARBON MONOXIDE HYDROGENATION. ADVISOR: ASST. PROF. PRASERT REUBROYCHAROEN, D.Eng., 79 pp.

ZSM-5 synthesis on electrospun silica fiber for carbon monoxide hydrogenation reaction (CO hydrogenation reaction) was prepared by hydrothermal process and characterized by XRD, SEM, EDX, BET, and TPR technique. The influencing parameters of ZSM-5 deposition on electrospun silica fiber were studied by variation of pH in the solution (8-10), hydrothermal time (24-72 h), hydrothermal temperature (170-190 $^{\circ}$C), and Si/Al ratio (20-80). The results indicated that the suitable condition for ZSM-5 preparation on electrospun silica fiber was at pH 9, hydrothermal conditions 180 $^{\circ}$C for 24 h. An increasing in Si/Al ratio from 20 to 80 results in increase ZSM-5 deposition on electrospun silica fiber. The catalytic properties of electrospun silica fiber, ZSM-5 on electrospun silica fiber (Si/Al ratio from 20-80), commercial silica (porous), and commercial ZSM-5 (porous) with 10%wt of Co were studied by CO hydrogenation reaction with H_2:CO ratio of 2:1, space velocity 75 ml/min/g, and reaction temperature 280 $^{\circ}$C. The results indicated that increasing of Si/Al ratio from 20 to 80 leads to increasing of %CO conversion from 34.29 to 42.99% whereas %CH_4 selectivity tends to decrease from 93.10 to 88.33. The ZSM-5 synthesized on electrospun silica fiber with Si/Al ratio of 80 yielded the highest CO conversion (42.99%) and Si/Al ratio of 20 yielded the highest CH_4 selectivity (93.10%).

Field of Study: Petrochemistry and Polymer Science
Academic Year: 2013

Student's Signature .....
Advisor's Signature .....

ACKNOWLEDGEMENTS

This research would not have been possible without the support of many people.I would like to express the deepest appreciation to my advisor, Asst.Prof.Dr. Prasert Reubroycharoen who was abundantly helpful and offered invaluable assistance, support and guidance for my Master's degree study. I would also like to express my gratitude to thesis committee members, Prof. Dr. Pattarapan Prasassarakich, Assoc. Prof. Dr. Wimonrat Trakarnpruk and Asst. Prof. Dr. Chanatip Samart without whose knowledge and assistance this study would not have been successful. Special thank to Mr. Wittawat Thawornsuk, Miss Natthawan Thakonkiattikun and Mr. Panya Wattanapaphawong and all of thesis group members for sharing the literature and invaluable assistance. I would like to thank Mr. Supote Puthawong for supporting the analytical instruments. I would also like to convey thanks to the Department and Faculty for providing the financial means and laboratory facilities. Finally, I wish to express my gratitude to my beloved families; for understanding and endless love, through the duration of my studies.

CONTENTS

Page

Page

TABLE CONTENTS

Page

Page

CONTENT OF FIGURES

Page

Page

Page

CHAPTER I

INTRODUCTION

1.1 Statement of problem

ZSM-5 is the medium pore zeolite that composes of three dimensional structures of silica and alumina. Due to its acidity, thermal stability, selectivity and porous properties, it can be used as catalyst for many chemical processes for example dewaxing, xylene isomerization, benzene alkylation and CO hydrogenation [1, 2]. In packed bed reactor, ZSM-5 can be used in several forms such as powder, spheres or extrudates but these forms generate high pressure drop, poor mass and heat transfer [3, 4]. Thus the fibrous form catalyst is an attractive choice because it has not only flexibility and endless forms which possible to adjust its shape to fit into the gas channel but also provides low resistance to flow of gas and short diffusion distance [5, 6]. However, ZSM-5 cannot directly form into fiber by electrospinning method because it requires hydrothermal step for synthesis. Thus the electrospun silica fiber was applied as the support for ZSM-5 due to its thermal stability, hydrophilic properties and having silanol group that is compatibility with zeolite surface [5, 7].

In this research, the experiment divides into two sections which are ZSM-5 synthesis on electrospun silica fiber and catalytic testing with CO hydrogenation reaction. The first section has studied the parameters of pH, hydrothermal temperature, hydrothermal time and Si/Al ratio that effect to growing characteristic of ZSM-5 crystal on electrospun silica fiber and dissolution of fibrous support. The second section, the catalysts have been loaded with 10%wt of Co and have studied the catalytic performance of catalyst with various supports which are electrospun silica fiber, commercial silica (porous), commercial ZSM-5 (porous) and ZSM-5 on electrospun silica fiber with different Si/Al ratios.

1.2 Objective

1.2.1 To synthesize ZSM-5 on electrospun silica fiber.

1.2.2 To study parameters that affect ZSM-5 synthesis on electrospun sililca fiber.

1.2.3 To study the catalytic performance in CO hydrogenation reaction.

1.3 Scope of research

1.3.1 Synthesize ZSM-5 on electrospun silica fiber

1.3.2 Study the parameters of ZSM-5 synthesis on electrospun sililca fiber by variation of pH of solution (8, 9 and 10), hydrothermal temperature (170, 180 and 190 ℃), hydrothermal time (24, 48, 60 and 72 h) and Si/Al ratios (20, 40, 60 and 80).

1.3.3 Study the catalytic performance in CO hydrogenation reaction by loading 10%wt Co on various supports which are electrospun silica fiber, commercial silica (porous), commercial ZSM-5 (porous) and ZSM-5 on electrospun silica fiber with different Si/Al ratios.

1.4 Expecteted outcome

1.4.1 ZSM-5 crystal is orderly and densely deposited on electrospun silica fiber.

1.4.2 The optimum condition for ZSM-5 synthesis on electrospun sililca fiber is obtained.

1.4.3 The prepared catalysts can be applied with CO hydrogenation reaction.

CHAPTER II

THEORY AND LITERATURE REVIEWS

2.1 ZSM-5

2.1.1 ZSM-5 structure

ZSM-5 or Zeolite Socony Mobil–5 is the microcrystalline aluminosilicates zeolite that was first synthesized by Argauer and Landolt in 1972 [1]. Their primary structures consist of TO_4 which T is Si^{4+} and Al^{3+} ion and each O^{2-} is linked between T atoms lead to three-dimensional framework of TO_2 as showns in Fig. 2.1. In this case, silica framework will give uncharged unit whereas aluminium has a negative charge so it requires positive charge to neutralize its overall framework.

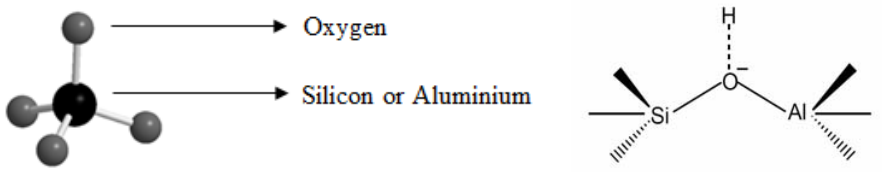

Fig. 2.1 Primary structure of ZSM-5 [8].

When these primary structures are linked together by oxygen, the pentasil secondary building units ($T_{12}O_{20}$) will occur that compose of eight five-membered rings then they will form into pentasil chains. Several pentasil chains are formed together via oxygen bridges resulting in complete structure of ZSM-5 which contains 96 T-atoms and 192 O-atoms [9].

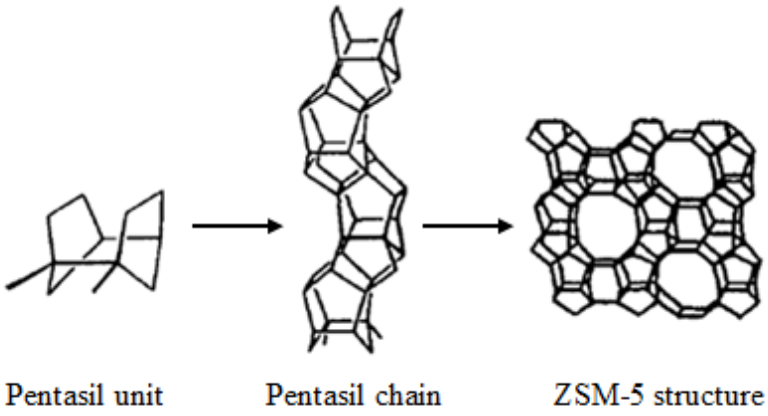

Fig. 2.2 Secondary building unit and complete structure of ZSM-5 [6].

ZSM-5 has two perpendicular channel systems as shown in Fig. 2.3; the intersecting straight channels are parallel to [010] plane with dimensions 0.55 x 0.51 nm while the sinusoidal channels are parallel to [100] plane and their dimensions equal to 0.56 x 0.54 nm [7]. The chemical formula of ZSM-5 is $M_{x/n}$ $[(AlO_2)_x(SiO_2)_y]$ $.wH_2O$ which n is the valence of the charge balancing cation M, w is the number of water molecule per unit cell and y/x is the ratio of Si/Al that are more than 5.

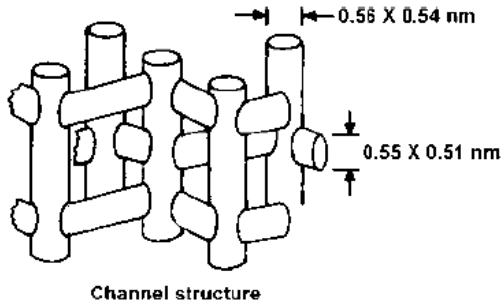

Fig. 2.3 ZSM-5 pore systems [10].

2.1.2 ZSM-5 synthesis

ZSM-5 is generally synthesized via hydrothermal conditions [11, 12]. The silica source, alumina source, organic template and water are mixed under high pH to form supersaturated solution and are converted into microporous crystalline aluminosilicate at elevated temperature. The mechanisms of zeolite synthesis were proposed by David and Lobo in 1982 which are solution-mediate transport mechanism and solid phase transport mechanism. The prepared solution from the first mechanism is lack of hydrogel (solid phase), the hydrated species are surrounded by silicate and aluminate then these molecules will be condensed and form into zeolite crystals and as shown in Fig. 2.4. The second mechanism on Fig. 2.5 describes rearrangement of solid hydrogel to form zeolite structure.

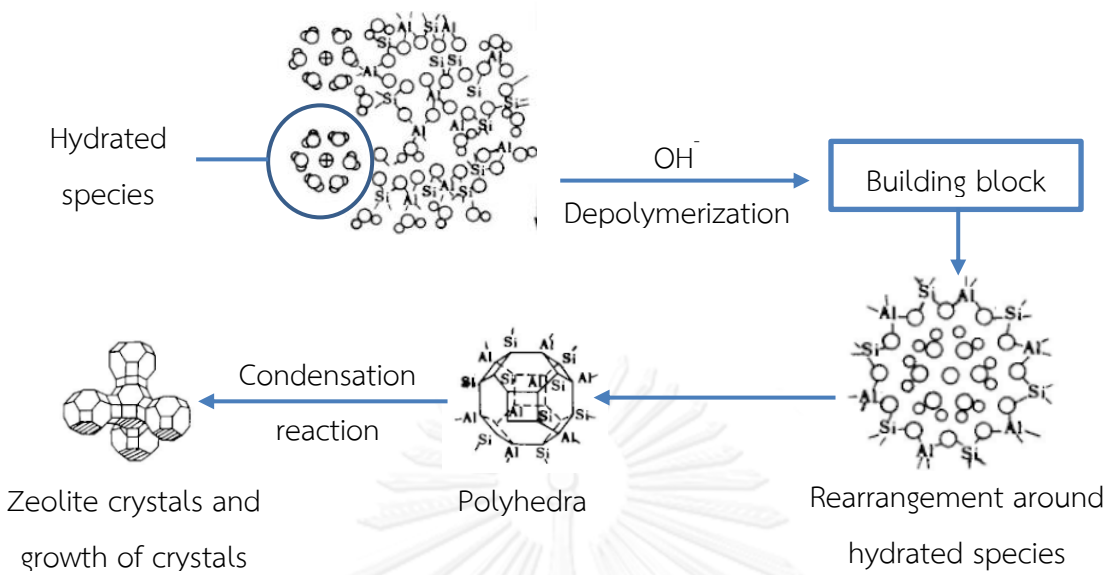

Fig. 2.4 Solution-mediate transport mechanism [11].

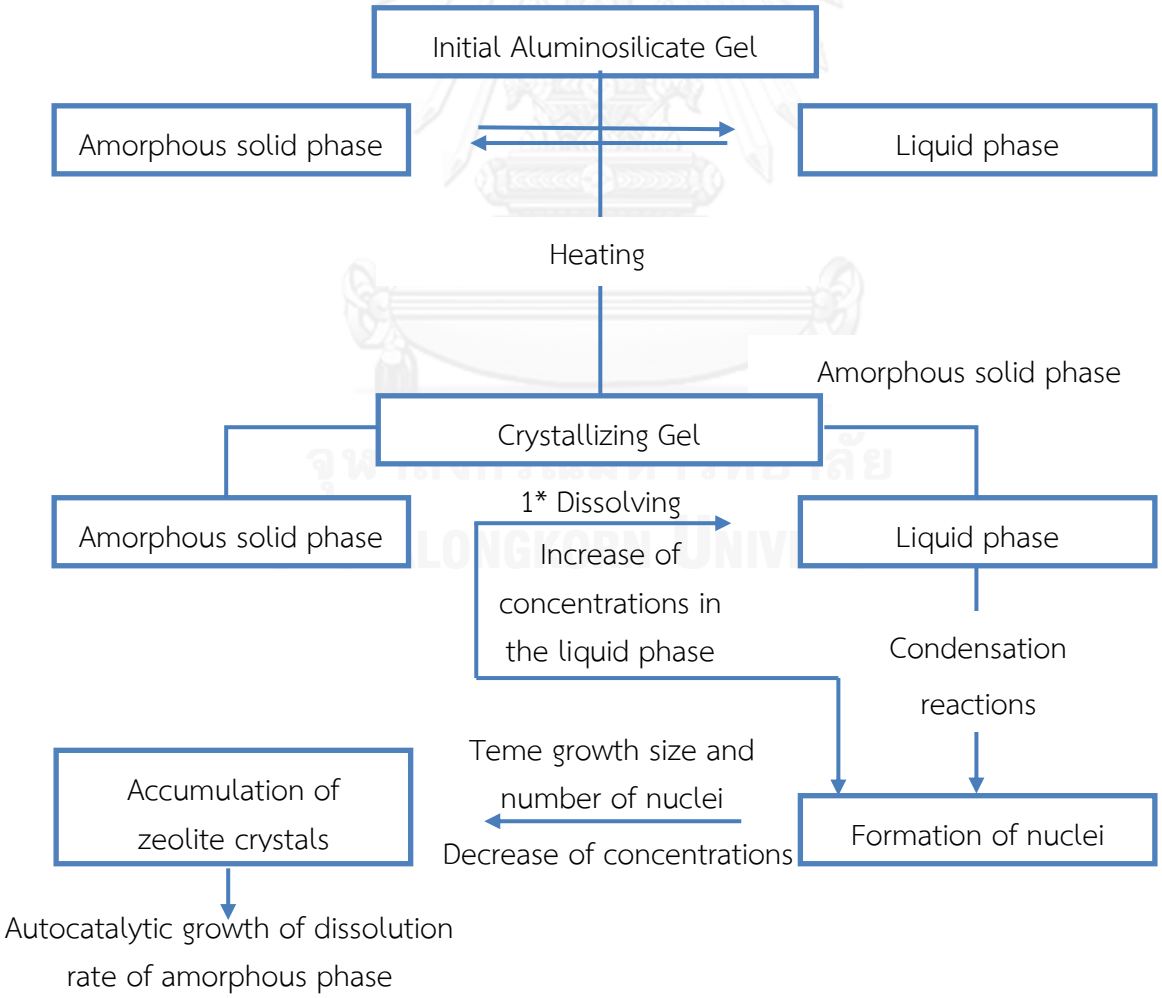

Fig. 2.5 Solid phase transport mechanism [11].

2.1.2.1 The factors affect to zeolite synthesis

2.1.2.1.1 Chemical composition

Molar composition is generally presented in forms of oxide formula, SiO_2, Al_2O_3, M_xO, N_yO, R, and H_2O where M and N are alkaline metal ions and R represents organic template. These compositions have greatly affected to zeolite synthesis as given in Table 2.1.

Table 2.1 Primary influences of compositions of the reaction mixture [8].

Mole Ratio	Primary Influence
SiO_2/ Al_2O_3	Framework composition
H_2O / SiO_2	Rate, crystallization mechanism
OH^-/ SiO_2	Silicate molecular weight, OH^- concentration
Na^+/ SiO_2	Structure, cation distribution
R_4N^+/ SiO_2	Framework aluminum content

2.1.2.1.2 Aging

Aging of hydrogel can reduce the induction time by increasing number of nuclei and rate of crystallization. Cundy and coworker [13] studied the effect of aging time on the crystallization of TS-1 and concluded that long period of aging time resulted in increasing the numbers of nuclei, therefore particle size tended to decrease. Rosilda [14] reported the effects of the aging temperature (25-180 °C) on the synthesis of nanocrystalline ZSM-5; they concluded that aging at high temperature can increase the particle size.

2.1.2.1.3 H_2O content for zeolite synthesis

Water content for zeolite synthesis [15] acts as solvent to promote mixing, transport of materials, encourage the nucleation and crystal growth. Moreover, it plays role as stabilizer of zeolite structure by filling the pores and forming a type of solid solution. Normally, the dilution of the synthetic mixture leads to lower supersaturation and earns the large crystals.

2.1.2.1.4 Crystallization Temperature and time

Zeolite synthesis under high temperature leads to increasing of nucleation rate, crystal growth rate and larger crystals have been obtained. Bhardwaj et al. [16]synthesized zeolite by varying the crystallization temperature between 75°C to 150°C. The amorphous phase was observed when the crystallization temperatures are lower than 150°C. Crystallization time is also a parameter for zeolite synthesis. As the report of Reza et al.[17], they prepared nano ZSM-5 at different crystallization times (72, 96 and 120 h) and concluded that longer time for crystallization, crystallinity and crystal size tend to increase, due to increase in crystals nucleation and growth rate.

2.1.2.1.5 pH

pH has the effect to supersaturation of silicate and aluminate species, kinetics, morphology, shape, size, and crystallinity of zeolite. The pH is influenced by the reactants, concentrations/ratios, temperature and time. An increase in pH will accelerate crystal growth and a shortened induction period before viable nuclei are formed.

2.1.2.1.6 Template

Template is the organic or inorganic bulky cations that use as spaces filler of zeolite structure. It encourages the formation of zeolite lattice by gelation, nucleation and decrease chemical potential (hydrogen-bonds, electrostatic and Van der waals force) of the lattice formed by the inclusion of the templates during zeolite synthesis.

2.1.3 Applications

Due to thermal stability, acidity, high surface area and shape selective properties of ZSM-5 thus it is appropriate to use as the support or catalyst in refineries and petrochemical process that summarizes in table 2.2.

Table 2.2 Industrial applications of ZSM-5 as the catalyst [18]

Process	Catalyst	Products
Catalytic cracking	Re-Y, US-Y, ZSM-5	Gasoline, fuels
Alkylation of aromatics	ZSM-5, Mordenite	p-xylene, ethyl-benzene, styrene
Xylene isomerization	ZSM-5	p-xylene
Catalytic dewaxing	Mordenite, ZSM-5+Ni nobel metals	Improvement of cold flow properties
Fischer–Tropsch synthesis	ZSM-5+Co,Fe, Ni	Synthesizing of hydrocarbon from synthesis gas

2.2 Silica fiber

For several years ago, many researches paid an attention to the fibrous form of silica because it can apply in various applications like reinforcement materials and biosensing. Furthermore, it also uses as the support for packed bed reactor systems which can provide low pressure drop and improve mass transfer in the reactor [19], [20]. The fibrous form of silica can be prepared via sol-gel and electrospinning process which are described in below.

2.2.1 Sol-gel process

Sol-gel [21] is the process for preparing solid materials from solution. Sol is a colloid suspension of solid particle in a liquid and gel is a three dimensional solid network which pores are filled with other substances. In general, there are two main reactions which are hydrolysis and condensation. The starting materials are usually organometallic substance in form of $M(OR)_n$ where M is metal with valence n, R is alkyl group with formula C_xH_{2x+1}. An example is sol-gel polymerization of tetraethoxysilane. The reaction proceeds via a series of condensation reactions that converts the tetraethoxysilane into $Si(OH)(OC_2H_5)_3$, $Si(OH)_2(OC_2H_5)_2$, $Si(OH)_3(OC_2H_5)$ and $Si(OH)_4$ then Si-O-Si linkages are formed by condensation reaction and generate the polymer solution.

Hydrolysis:

$$Si(OC_2H_5)_4 + H_2O \rightarrow Si(OH)(OC_2H_5)_3 + C_2H_5OH$$
$$Si(OH)(OC_2H_5)_3 + H_2O \rightarrow Si(OH)_2(OC_2H_5)_2 + C_2H_5OH$$
$$Si(OH)_2(OC_2H_5)_2 + H_2O \rightarrow Si(OH)_3(OC_2H_5) + C_2H_5OH$$
$$Si(OH)_3(OC_2H_5) + H_2O \rightarrow Si(OH)_4 + C_2H_5OH$$

Condensation:

$$(OH)_3SiOH + OHSi(OH)_3 \rightarrow (OH)_3Si\text{-}O\text{-}Si(OH)_3 + H_2O$$

or

$$(OH)_x(OR)_ySi\text{-}O\text{-}Si(OH)_v(OR)_w \rightarrow (OH)_x(OR)_ySi\text{-}O\text{-}Si(OH)_v(OR)_w + ROH$$

where x+y = v+w = 3

2.2.2 Electrospinning

Electrospinning or electrostatic spinning is a fabrication process that was first created in 1934 [22]. This process composes of a syringe pump that helps to eject polymer solution, needle, metal collector and high voltage supply as shown in Fig. 2.6. When the high voltage supply generates electric field between two electrodes, needle and metal collector, will bear the opposite electrical charge resulting in driving of polymer jet like Taylor cone into the collector [23]. During the ejection process, the charge on polymer jet was neutralized by exposure to ion in the air or contact with the collector. Simultaneously, the solvent will evaporate and form into solid fiber. The electrospun fiber is having diameters ranging from several microns down to lower than 100 nm. Generally, the fiber morphology and their diameters are depending on polymer solution properties (viscosity, conductivity, surface tension), ambient parameters (temperature, humidity, and air velocity) and process parameters (flow rate, applied voltage, distance between tip and collector) [24, 25].

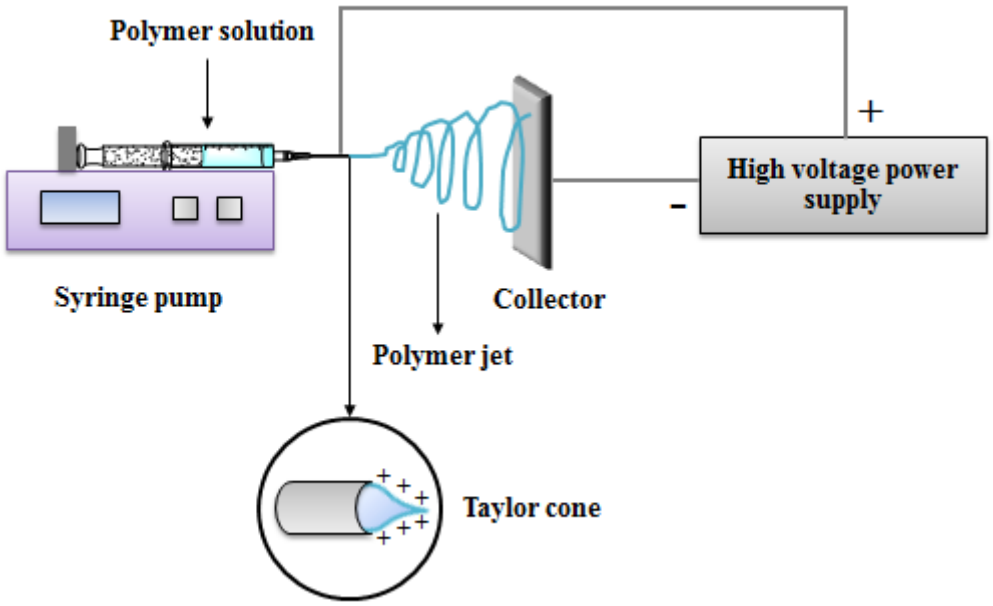

Fig. 2.6 The diagram of electrospinning process [26].

2.2.2.1 The influence parameters for electrospinning process

2.2.2.1.1 Viscosity/concentration

The effect of viscosity was studied by Sakai et al. as shown in Fig. 2.7 [27]. At lower solution viscosity/polymer concentration, the polymer jet is plenty of solvent causing droplet and beaded formation on the collector. In addition, the presence of junctions and bundles has been found. Increasing viscosity or polymer concentration generates homogeneous fiber with lower beads and junctions, the diameter of fiber also increases. Too high polymer concentration, the droplet dries out easily and clogs up at the tip before forming polymer jet. Therefore the electrospinning process is interrupted.

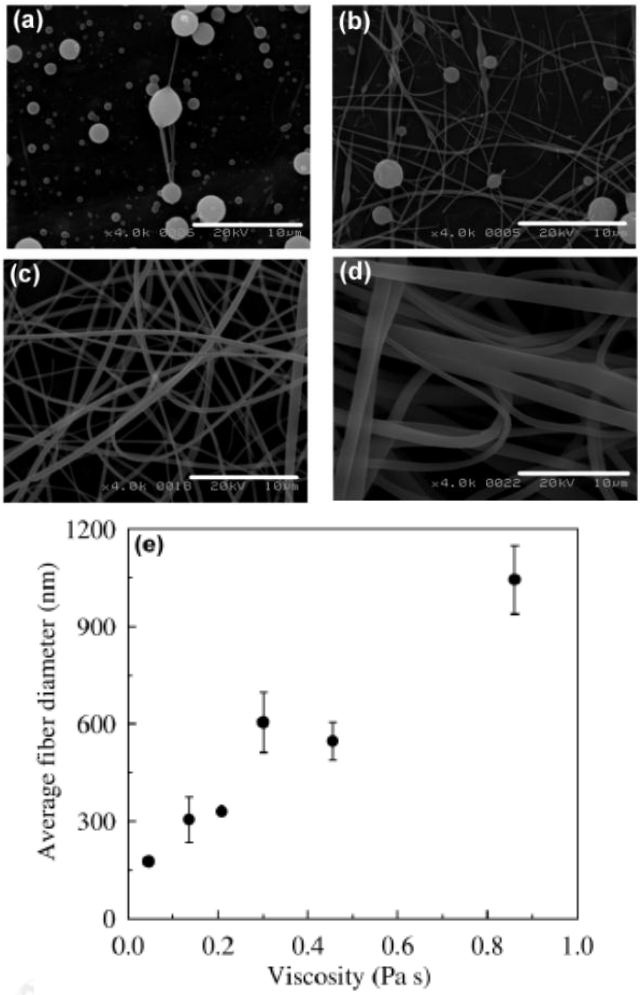

Fig. 2.7 SEM image of electrospun silica fiber with various viscosities (a) 0.03 (b) 0.05 (c) 0.14 (d) 0.86 Pa s and (e) average fiber diameters of silica fiber.

2.2.2.1.2 Conductivity

The conductivity depends on solution types. Using nonionic surfactant like tetrachloromethane leads to reducing of conductivity and beads formation has been found. Increasing solution conductivity, using alcohol and volatile salt additive, generates smoother fiber with fewer beads. Small ionic surfactant can increase charge density and mobility thus the polymer jet has more elongational force resulting in smaller fiber.

2.2.2.1.3 Surface tension

To initiate electrospinning process, the charges on polymer solution must be high enough to outdo the surface tension that will lead to stretching of polymer jet.

Thus the surface tension is also influencing parameter that controls spinning ability. With increasing surface tension causes beads forming on the fiber. Pirzada et al. prepared hybrid electrospun silica–PVA nanofiber with various ratios [28]. They used PVA for increasing number of entanglement in the silica solution resulting in increasing of surface tension. The proper silica to PVA ratio provides fiber with no beads and narrow sized distribution.

2.2.2.1.4 Flow rate

Decreasing flow rates produces smaller fiber. Too high flow rate lead to increase speed ejection, beads and junctions will form because fiber still wet when it reach to the collector.

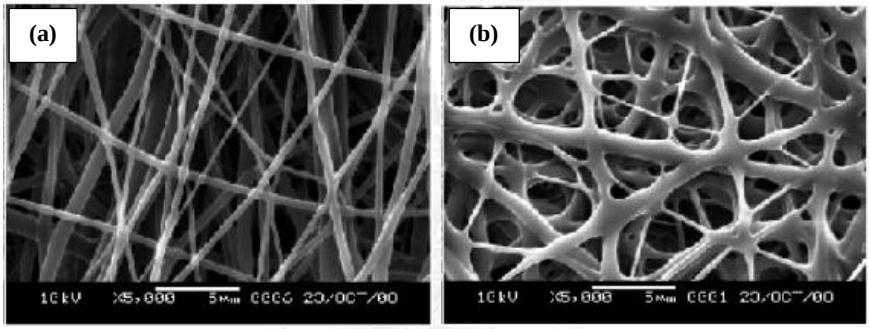

Fig. 2.8 SEM images of electrospun PLGA nanofiber with flow rates (a) 0.5 and (b) 2ml/h [29].

2.2.2.1.5 Applied voltages

Adding applied voltages causes the increasing of charges density on polymer jet thus the stretching force also increases, the smaller fiber is produced. Too high voltages can decrease the Taylor cone at the tip thus the polymer jet is not stably stretched resulting in many beads on fiber.

2.2.2.1.6 Tip to collector distance (TCD)

Increasing in tip to collector distance can produce smaller diameter and the fiber have more enough time to dry before getting to the collector.

2.2.2.1.7 Ambient parameters

The temperature and humidity are the ambient parameters for electrospinning process. As increasing temperature cause to decrease in viscosity of

polymer sol and yield smaller fiber diameter. The increasing of humidity effects to pores forming on fiber surface and brings about pore agglomeration.

2.2.3 Silica support for zeolite

Silica can be used as the support for various catalysts including zeolite due to the presence of thermal stability, hydrophobic properties and high amount of OH group that are compatible with zeolite. However, silica may be less stable under zeolite synthesis condition so it requires the suitable condition to prevent dissolution of the support [3].

2.3 Carbon monoxide hydrogenation process (CO hydrogenation process)

CO hydrogenation is the process to convert the aliphatic hydrocarbon from synthesis gas by using group VIII metal like cobalt, iron, ruthenium or nickel as the catalyst. In case of cobalt and iron, the reaction temperature is ranging between 200 to 300 °C and pressure 1 to 10 bars. The products from this process composed of linear hydrocarbons, branched hydrocarbons and oxygenated products however the major products are linear paraffin and α-olefin. The total reactions for CO hydrogenation are shown in table 2.3 [30].

Table 2.3 The total reactions of CO hydrogenation.

Main reactions	
Paraffin	$(2n+1)\ H_2 + nCO \rightarrow C_nH_{2n+2} + n\ H_2O$
Olefin	$2nH_2 + nCO \rightarrow C_nH_{2n} + n\ H_2O$
Water gas shift reaction	$CO + H_2O \rightarrow CO_2 + H_2$
Side reations	
Alcohols	$2nH_2 + nCO \rightarrow C_nH_{2n+2}O + (n-1)H_2O$
Boudouard reaction	$2CO \rightarrow C + CO_2$
Catalyst modifications	
Catalyst oxidation/reduction	a. $M_xO_y + yH_2 \rightleftharpoons yH_2O + xM$ b. b. $M_xO_y + yCO \rightleftharpoons yCO_2 + xM$
Bulk carbide formation	$yC + xM \rightleftharpoons M_xC_y$

2.3.1 Cobalt catalyst for CO hydrogenation

Cobalt and iron are commercially used for CO hydrogenation. Although cobalt has higher prices but it is about 3 times more reactive compared with iron. Moreover it provides longer lifetime and higher hydrogenation activity thus they tend to produce higher yields of high molecular weight linear alkanes and much less oxygenates. Furthermore, it is not inhibited by water, resulting in a higher productivity at a high synthesis-gas conversion. Due to its low water–gas shift activity therefore only small amounts of CO_2 can be found in the reactor at any given time. Normally, the prepared cobalt catalyst is presented in the form of metal oxide (Co_3O_4) thus reducing in H_2 at temperatures between 200 and 500 °C is required to activate the catalyst in the form of Co^0. There are two-steps of reduction which are $Co_3O_4 \rightarrow CoO$ and $CoO \rightarrow Co^0$.

2.3.2 CO hydrogenation mechanism

The mechanism for CO hydrogenation can be concluded as the following steps:

1) Reactant adsorption

$CO + s \rightleftharpoons COs$

$COs + s \rightleftharpoons Cs + Os$

$H_2 + 2s \rightleftharpoons 2Hs$

2) Surface reactions

Water formation

$Os + Hs \rightleftharpoons HOs + s$

$HOs + Hs \rightleftharpoons H_2O + 2s$

$Os + H_2 \rightleftharpoons H_2O + s$

Chain initiation

$Cs + Hs \rightleftharpoons CHs + s$

$CHs + Hs \rightleftharpoons CH_2s + s$

$CH_2s + Hs \rightleftharpoons CH_3s + s$

or

$COs + H_2 \rightleftharpoons CHOHs$

$CHOHs + H_2 \rightleftharpoons CH_2s + H_2O$

Methanation

$CH_3s + Hs \rightleftharpoons CH_4 + s$

Chain growth

$C_nH_{2n+1}s + CH_2s \rightleftharpoons C_{n+1}H_{2n+3}s + s$

Hydrogenation to paraffin

$C_nH_{2n+1}s + Hs \rightleftharpoons C_nH_{2n+2} + 2s$

β-Dehydrogenation to olefin

$C_nH_{2n+1}s \rightleftharpoons C_nH_{2n} + Hs$

3) Chain termination and products desorption

Chain termination occurs by detraction of hydrogen to an olefin or addition of a CH_3 species or hydrogen to form a paraffin then the products desorb from the catalyst as shown in Fig. 2.9

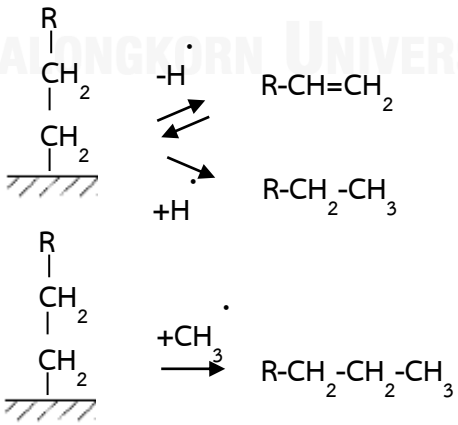

Fig. 2.9 An example of chain termination and products desorption [30].

4) Reactant readsorption

After removing of the products from catalyst surface, the readsorption of reactant will take place and initiates hydrocarbon chain.

5) Water-gas shift reaction

Water–gas shift mechanism over cobalt catalyst occurs via a reactive formate intermediate that shown in Fig. 2.10. The adsorption of hydroxy species or water and carbon monoxide lead to formation of formate species and the hydroxy intermediate can be formed by the decomposition of water. The formate species a can be reduced to carbon dioxide.

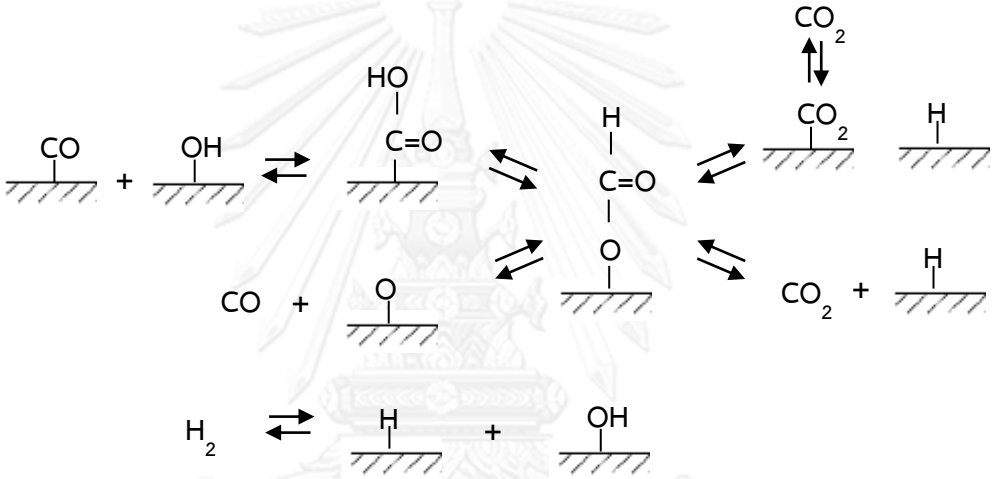

Fig. 2.10 Water–gas shift reaction mechanism via formate species [30].

2.3.3 The influence parameters

2.3.3.1 Temperature

Increasing of temperature leads to lower carbon number of the products. As the report of Choosri et al. [31], they studied the performance of Co/SiO_2 catalyst for Fischer–Tropsch synthesis (FTS) in slurry phase reactor and varied the reaction temperature from 220 to 260 °C. They concluded that the reaction temperature has strongly affected to the performance of the catalyst towards FTS. Increasing temperature resulted in higher CO conversion to hydrocarbon and produced more spread of carbon numbers. The lower carbon number also obtained.

2.3.3.2 Partial pressure of H_2 and CO

When increase the total pressure, the product selectivity shift to heavier product. High H_2/CO ratios result in lighter hydrocarbons and lower olefin content.

Sarkari et al. [32] studied the effect of H_2/CO ratio (1.0-3.0) by using alumina supported iron-nickel as the catalyst for FTS. The conclusion is lower CO partial pressure resulting in a lower concentration of adsorbed CO, so that more H_2 can be adsorbed and dissociated. The lighter hydrocarbon products will be generated.

2.3.3.3 Space velocity

The influence of space velocity of synthesis gas has been investigated over calcium-promoted Co/alumina catalyst by Osa et al. They found that the increase of space velocity results in a decrease of CO conversion. The selectivity of C_1-C_4 light hydrocarbons, CO_2 and olefin tend to increase [33].

2.3.3.4 Time on stream

With increasing time on stream results in catalyst deactivation due to poisoning, re-oxidation of cobalt, formation of surface carbon species, carbidization, surface reconstruction, metal–support solid state reactions and attrition [34]. Therefore, the activity and selectivity of hydrocarbon products may lower [26]. Karre et al. [35] investigated time on stream of FTS reaction via ZSM-5/iron-based activated-carbon-supported catalyst. The catalyst activity slowly dropped up to 240 h because of a decrease in iron carbide. The coke formation on ZSM-5 leads to decreasing the aromatic compound yield, and increasing olefin selectivity with time on stream due to reduction in oligomerization reaction.

2.3.3.5 Reduction of catalyst

The effect of reduction conditions was investigated with a precipitated iron Fischer-Tropsch catalyst by Dragomir and coworker [36], they concluded that catalyst reducing under H_2 resulted in increasing stability of catalyst with time on stream and generated more methane and gaseous hydrocarbons compared with the catalysts that were reduced with carbon monoxide or synthesis gas. Dai [37] studied the effect of reduction temperature and time. The increasing of reduction temperature and time, the lighter hydrocarbon products tended to increase and gave high CO conversion.

2.4 Literature reviews

CO hydrogenation reaction has recently been received considerable attention as an alternative method for synthesizing clean fuels from synthesis gas. Yanyong et al. [38] Steen et al. [39] and many research [40, 41] reported that Fe, Co, Ru are generally used as catalyst for CO hydrogenation reaction but Co is a good candidate due to high catalytic performance, high selectivity to long chain normal paraffins, low activity to water gas shift reaction (comparing to Fe) , low price (comparing to Ru). Co is normally deposited on high surface area support such as porous alumina, porous silica and ZSM-5 to obtain high metal dispersion [42]. Different types of support affects to metal dispersion, metal size and reducibility of catalyst. Silica support has weak metal–support interaction, high reducibility and generating long chain hydrocarbon products whereas alumina has strong metal support interaction, low reducibility and generating short chain hydrocarbon products.

Kang et al [43] studied Co supported catalyst for CO hydrogenation. They reported that support with higher acidity decrease the crystallite size of Co_3O_4 and conclude that high metal-support interaction shifts the reduction temperature to higher region. The activity of catalyst depends on the support which affects in crystal size, metal dispersion, reducibility and activity of Co species in CO hydrogenation reaction and C_{5+} selectivity was in order Co/SiO_2>Co/Al_2O_3>Co/TiO_2.

In case of ZSM-5 support, it has lower reducibility than silica support but it contains acid site that able to crack and isomerize hydrocarbon products into gasoline range as described in research of Yang et al [44, 45]

Yang et al. [45] synthesized core-shell like zeolite capsule catalyst by deposition of silicalite-1 onto Co/SiO_2 then synthesized ZSM-5 via hydrothermal process at 180 °C 24 hours to become a final layer. The obtained catalyst was named Co/SiO_2-Z-HT. The catalytic testing was investigated by FTS reaction and compared among Co/SiO_2-Z-HT, physically adhesive method (Co/SiO_2-Z-PA) and physically mixed ZSM-5/Co/SiO_2 (Co/SiO_2-Z-M) catalyst. All the tested catalysts displayed CO conversion over 90%, the major products composed of light hydrocarbon which were n-paraffin and isoparaffin. The CH_4 selectivity was ranging from 17.5-23.7%. Co/SiO_2-Z-PA provided the highest catalytic performance whereas Co/SiO_2-Z-HT gave lowest due to the zeolite overspreading on Co/SiO_2, the reactants and products are more difficult to react with Co. Moreover, there might be partial interaction between Co clusters with Brönsted acid site of zeolite which suppressed cracking activity during FTS reaction.

Although the porous support (silica porous, alumina porous and ZSM-5) has the advantage in high surface area but its drawback is poor mass transfer, poor heat transfer including high pressure drop that affect to catalytic performance [4]. The fibrous form catalyst is the good choices for improve these problems therefore it was paid attention in several years ago. As shown in research of Yodwanlop [46] and Louis [47]

Yodwanlop [46] prepared nano-electrospun silica fiber for FTS reaction by using TEOS, HCl, H_2O and ethanol as the precursors then studied parameters influencing to the fiber characteristic which are diameter of needle size (0.1 and 0.25 mm.), TCD (10 - 20 cm.) and applied voltage (10-20 kV). The obtained fiber was dried in oven at 110 °C for 24 h then loaded with 10-20 %wt. of Co and calcined at 400 °C for 2 h. The catalytic performance was investigated under the temperature varying from 240 to 280 °C. In the electrospinning step, adjusting needle size from 0.25 to 0.1 mm. lead to smaller diameter of fiber but the silica solution also clogged up at the needle easily. Moreover, the lower yield of electrospun fiber was found comparing with 0.25 mm. The appropriate TCD and applied voltage are 15 cm. and 15 kV which offered the smallest fiber with average diameter 329 nm. FTS reaction concluded that the 10% wt. of Co yielded the highest FTS product selectivity and increasing in temperature to 280 °C gave the highest catalytic stability and selectivity.

Louis et al. [47] prepared ZSM-5 on glass fibrous support with 3 different methods that were synthesized in alkaline media without silica source, synthesized in alkaline media without silica source and synthesized with fluoride method. All synthesized catalysts were characterized by BET SEM and XRD and the catalysts were tested with gas-phase partial oxidation of benzene by N_2O to phenol. The fluoride-containing zeolite catalysts exhibited the highest performance with benzene conversion over 20% and 98% selectivity of phenol.

Generally, ZSM-5 is produced by hydrothermal process and cannot directly produce into fibrous form. Therefore the fibrous support is required for ZSM-5 deposition. As described in chapter I, we choose silica as the support for ZSM-5 due to thermal stability, compositional compatibility. The fibrous form of silica support was prepared by electrospinning technique as the research of Choi [48]

Choi [48] prepared silica nanofiber from 1TEOS: 0.01HCl: $2H_2O$: 2EtOH. The polymer solution was stirred and heated at 80 °C for 30 min. The distance between the tip to collector was 10 cm and the applied voltage was ranging from 10 to 16 kV. High applied voltage led to the shifting of smaller diameter distribution. The diameter was mostly ranging between 200-600 nm. FTIR results revealed 795, 950, and 1058

cm^{-1} belonging to Si-O vibration and showed the OH-vibration peak at 3390 cm^{-1}. This can conclude that TEOS was mostly hydrolyzed and the ethoxy group changed into the silanol group. The XRD pattern indicated the characteristic peak of amorphous silica. TGA results showed weight loss approximate to 6.7% at 200 °C owing to evaporation of solvent and at 800 °C the weight loss was about 12% due to self-condensation reaction of silanol group.

CHAPTER III

METHODOLOGY

3.1 Equipment and instruments

3.1.1 Equipment for catalyst preparation

1) Beaker (Teflon) 100 ml
2) Beaker (glass) 250 and 500 ml
3) Dropper
4) Pipette 5 and 10 ml
5) Spatula
6) Forceps
7) Glass rod
8) Cylinder 50 ml
9) Separating funnel
10) Wash bottle
11) Crucible
12) Watch glass
13) Brush
14) Rubber pipette bulb
15) Clamp
16) Magnetic bar and Magnetic stirrer
17) Water bath
18) Syringe 3 ml
19) Needle with diameter 0.55 mm
20) Aluminum foil
21) Teflon lined stainless steel reactor
22) Wrench

3.1.2 Instruments for catalyst preparation

1) Metal collector size 20 x 20 cm
2) High voltage supplier
3) Syringe pump
4) Hydrothermal machine
5) Muffle furnace

6) Oven
7) Desiccator

3.1.3 Instruments for catalyst characterization

1) Scanning electron microscope (SEM)
2) Energy Dispersive X-ray Fluorescence (EDX)
3) X-ray Diffractometer (XRD)
4) Surface area and porosity analyzer (BET)
5) Temperature programmed reduction (TPR)

3.1.4 Equipment and instruments for catalytic testing by CO hydrogenation reaction

1) Quartz wool
2) Silicone tube
3) Fixed bed reactor
4) Tube furnace
5) Temperature controller
6) Thermocouple
7) Mass flow controller
8) Gas Chromatograph, Shimadzu GC-2014

3.2 Reagent and Chemicals

1) Tetraethyl orthosilicate (TEOS) ≥ 99.0%, Sigma-Aldrich
2) Aluminium nitrate ($Al(NO_3)_3.9H_2O$), Univar
3) Tetrapropyl ammonium hydroxide (TPAOH) 1 M, Sigma-Aldrich
4) Ethanol (C_2H_5OH) ≥ 99.9%, CARLO ERBA
5) Hydrochloric acid (HCl) 37.0%, QRëC
6) Nitric acid (HNO_3) 70%, Sigma-Aldrich
7) Glycerol 99.5%, QRëC
8) $Co(NO_3)_2.6H_2O$, Univar
9) Deionized water
10) Helium gas 99.99%, Praxair
11) Nitrogen gas 99.99%, Praxair
12) Hydrogen gas 99.99%, Praxair
13) Gas mixture of nitrogen 95% and hydrogen 5%, Praxair

14) Gas mixture of ethane 1%, carbon dioxide 1.01%, ethylene 1%, methane 1.04%, carbon monoxide 1.02% and hydrogen 1% balanced in nitrogen, BOC scientific
15) Gas mixture of hydrogen 48%, carbon monoxide 48% balance in argon, BOC scientific

3.3 Experimental Procedure

3.3.1 Preparation of electrospun silica fiber

1) Mixed 18 ml of TEOS and 3 ml of DI water for 5 minutes then dropped 0.01 ml of HCl into the solution and continuously stirred for 5 minutes.
2) Added 9.72 ml of ethanol and stirred for 5 minutes following by stirred at 70 °C for 30 minutes. The silica solution was place in the room temperature until viscous then filled into the syringe and combined with the needle.
3) Installed the syringe on syringe pump then linked the wire from high voltage supplied to the collector and needle. The next was setting the conditions for electrospinning as follow: Tip to collector distance (TCD) 10 cm, needle size 0.55 mm, spinning rate 10 ml/h and applied voltage 15 kV. Under the electric field, the jet of silica solution was ejected in the form of nanofiber and deposited on the collector.
4) The obtained electrospun silica fiber was dried in oven at 110 °C for 12 hours and calcined at 400 °C for 2 hours.

3.3.2 Preparation of ZSM-5 on electrospun silica fiber

1) Calculated the amount of precursor with molar ratio 1TEOS: 0.25TPAOH: $xAl(NO_3)_3.9H_2O$: $80H_2O$ where x = 0.050, 0.025, 0.017 and 0.0125 to obtain Si/Al ratios 20, 40, 60 and 80.
2) Prepared silica source starting from adding a drop of 3M HNO_3 into DI water then added into TEOS and stirred at room temperature for 30 minutes followed by dropping of TPAOH and stirred at 60 °C for 30 minutes.
3) Prepared the alumina source by mixing $Al(NO_3)_3.9H_2O$, H_2O and TPAOH then stirred to get a clear solution. After that, the alumina source was added into silica source and stirred at 60 °C for 1 hour then stirred at room temperature for 2 hours and adjusted pH (8, 9 and 10) with HNO_3.

4) Prepared the solution with 1TEOS: 0.25TPAOH: 80H_2O as the procedure in the topic 3.3.2 choice 1) and dropped into electrospun silica and heated fiber at 60 ˚C for a few minutes.
5) Filled the silica fiber and loaded the prepared solution into teflon-lined hydrothermal reactor. Hydrothermal process was performed under the conditions 170-190 ˚C for 24-72 hours with 2 rpm. Rinsed the synthesized catalyst with deionized water, dried at 120 ˚C for 12 hours and calcined at 550 ˚C for 5 hours.

3.3.3 Preparation of Co on electrospun silica fiber and Co on ZSM-5 electrospun silica fiber support

1) Immersed 0.2 g of electrospun silica fiber in 20 ml of 2 M HNO_3 for 10 minutes then washed in DI water and dried in oven at 110 ˚C.
2) Prepared 10%wt of Co on fibrous support by dissolving $Co(NO_3)_2.6H_2O$ into DI water 10 ml and mixing with 2 ml of glycerol.
3) Impregnated $Co(NO_3)_2.6H_2O$ solution onto electrospun silica fiber and dried in oven at 110 ˚C, repeated this step until the solution was expended.
4) Dried the electrospun silica fiber again at 110 ˚C for 12 hours and calcined the fibrous catalyst at 400 ˚C for 2 hours.
5) Impregnated Co on ZSM-5 supported with electrospun silica fiber had the similar steps from 1) to 4) in the topic 3.3.3 but the fiber did not immerse in HNO_3.

3.3.4 Preparation of Co on commercial ZSM-5 (porous)

1) Calcined ZSM-5 at 550 ˚C for 5 hours
2) Impregnated 10%wt of Co on porous support by dissolving $Co(NO_3)_2.6H_2O$ into 10 ml of DI water.
3) Slowly dropped $Co(NO_3)_2.6H_2O$ into 0.2 g of commercial ZSM-5 and spread it out then dried in oven at 110 ˚C.
4) Repeated 3.3.4.3 until the solution was expended.
5) Dried in oven at 110 ˚C for 12 hours and calcined the fibrous catalyst at 400 ˚C for 2 hours.

3.3.5 Characterization of catalyst

1) Scanning electron microscope (SEM)

Morphology, crystal size and coating of ZSM-5 on fibrous support were studied using JOEL model JSM-6480LV Scanning electron microscope.

2) N_2 physisorption

Surface area and pore volume of ZSM-5 on electrospun silica fiber were measured by BET (Micromeritics, model: ASAP 2020)

3) X-ray Diffractometer (XRD)

XRD patterns of ZSM-5 on silica fiber and Co-ZSM-5/electrospun silica fiber were recorded by Bruker AXS model D8 Advance, equipped with Cu-Kα. The scanned angle (θ) was starting from 5° to 50° for ZSM-5 on electrospun silica and 5° to 80° for Co catalyst. The Co crystal size was calculated from Scherrer equation that showned in below.

$$\text{Average crystal size} = \frac{K\lambda}{\beta \cos\theta}$$

Where

K = Scherrer constant

λ = Wavelength of x-ray (Cu, Kα = 0.15406 Å)

β = Line broadening at half the maximum intensity (FWHM)

θ = Bragg angle

4) Energy Dispersive X-ray Fluorescence (EDX)

Elemental components in Co-ZSM-5/electrospun silica fiber were detected by Energy Dispersive X-ray Fluorescence (Shimadzu, model: EDX-720)

5) Temperature programmed reduction (TPR)

Reduction temperature and reducibility of catalyst were carried out using TPR. 0.1 g of catalyst was heated up to 100 °C with heating rate 10°C/min and flowed N_2 with flow rate 30 ml/min for 30 minutes to remove moisture and impurity. After this period, the N_2 flux was replaced by 5% of H_2 balanced with N_2. The temperature was heated from 100 to 800 °C with heating rate 3°C/min to reduce the catalyst. The percent of reduction of Co-ZSM-5/electrospun silica fiber can be calculated as following equation.

$$\% \text{ reduction} = \frac{H_2 \text{ consumption}_{measured}(mol)}{H_2 \text{ consumption}_{calculated}(mol)} \times 100$$

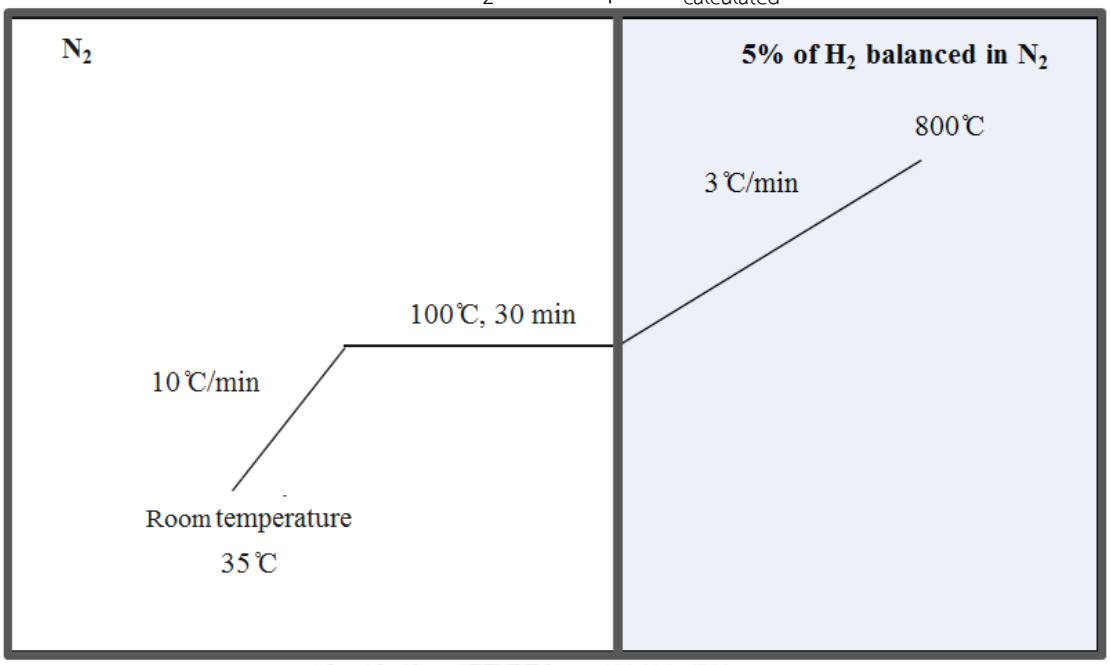

Fig. 3.1 Schematic of temperature heated up for TPR [46].

3.4 CO hydrogenation process

1) Packed 0.2 g of catalyst into a fix bed reactor.
2) Activated the catalyst by reducing under H_2 flow (space velocity 150 ml/min/g) at atmospheric pressure, 400 ˚C for 3 hours.
3) Flushed N_2 (space velocity 100 ml/min/g) into the reactor for 20 minutes to remove H_2
4) Set the temperature of furnace at 280 ˚C then passed H_2/CO with ratio 2:1, space velocity 75 ml/min/g for 20 minutes before analyzing.
5) Analyzed the gaseous products by GC with thermal conductivity detector. The GC conditions were shown in table 3.1.
6) Studied the parameters that affected CO hydrogenation reaction which are types of support (electrospun silica, commercial silica (porous), commercial ZSM-5 (porous) and ZSM-5 on electrospun silica fiber) and Si/Al ratios (20, 40, 60 and 80).

Table 3.1 The conditions for GC analysis.

Carrier gas	99.999 % of He
Column type	Unibead C
Injection temperature	120 ˚C
Column temperature	Temperature program 100 ˚C, 3.30 minutes 180 ˚C, 5.37 minutes (rate 15 ˚C /min)
Detector type	TCD
Detector temperature	180 ˚C

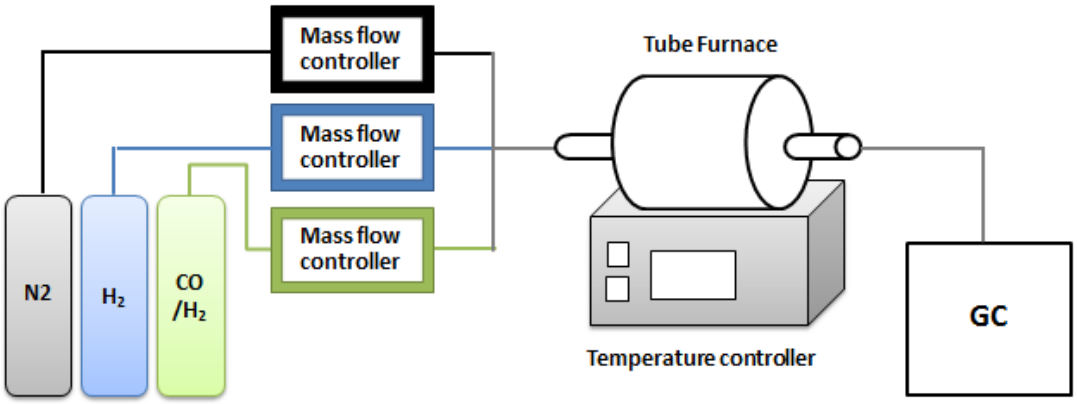

Fig. 3.2 Equipment and instrument diagram for CO hydrogenation reaction [46].

CHAPTER IV

RESULTS AND DISCUSSION

4.1 The study of supported materials

4.1.1 The properties of electrospun silica fiber

The SEM image in Fig. 4.1 showed the morphology of nonwoven electrospun silica fiber that was prepared by using needle size 0.55 mm, TCD 10 cm, applied voltage 15 kV and feed rate 10 ml/h. The obtained fiber was quite smooth. The size distribution of diameters are starting from 0.49 to 0.95 μm and mostly ranging between 0.60 to 0.71 μm with average diameter 0.68 μm that illustrated in Fig. 4.2.

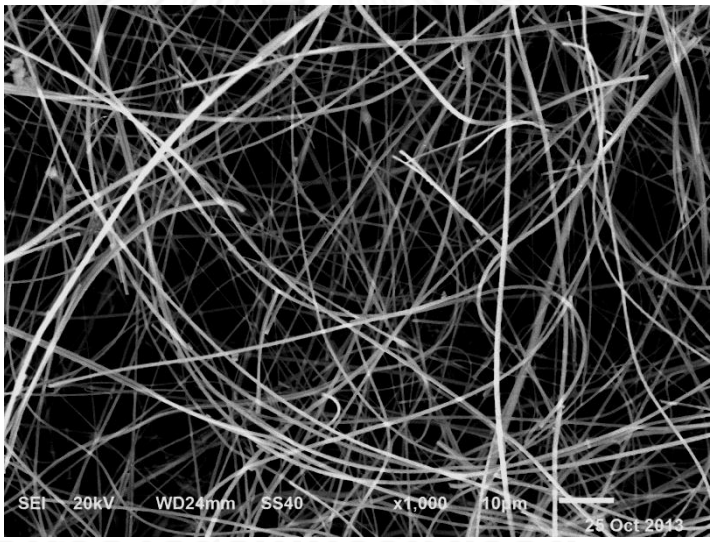

Fig. 4.1 SEM image of electrospun silica fiber prepared by using 0.55 mm of needle with TCD 10 cm, applied voltage 15 kV and spinning rate 10 ml/h.

The crystalline structure of electrospun silica fiber was investigated by using XRD pattern in Fig. 4.3 summarizing that the synthesized electrospun silica fiber exhibited the amorphous silica pattern [48, 49]. BET result indicated that the fiber is nonporous material due to its small surface area (3.80 m^2/g) and small pore volume (0.002 cm^3/g). However it presented the large pore size with 23.374 Å resulting from the inter-fiber void space.

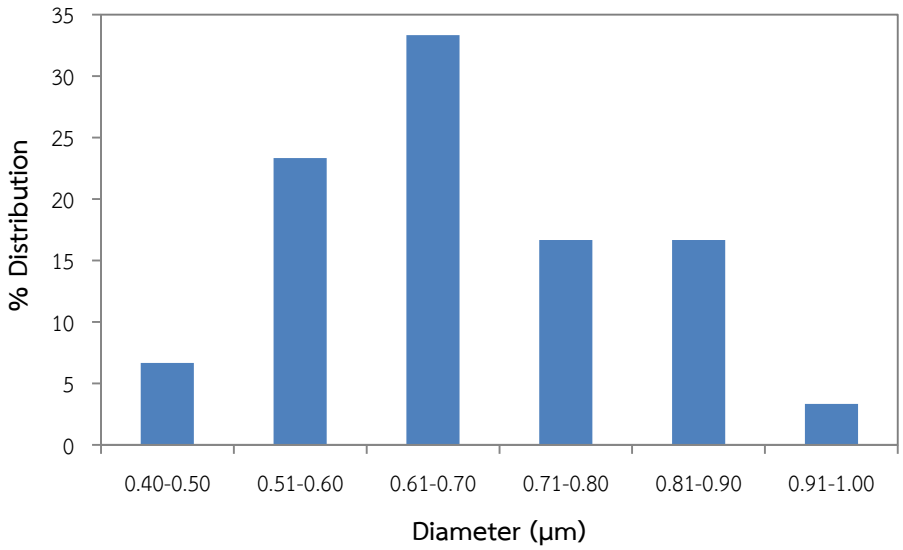

Fig. 4.2 Diagram of % distribution and diameter of electrospun silica fiber.

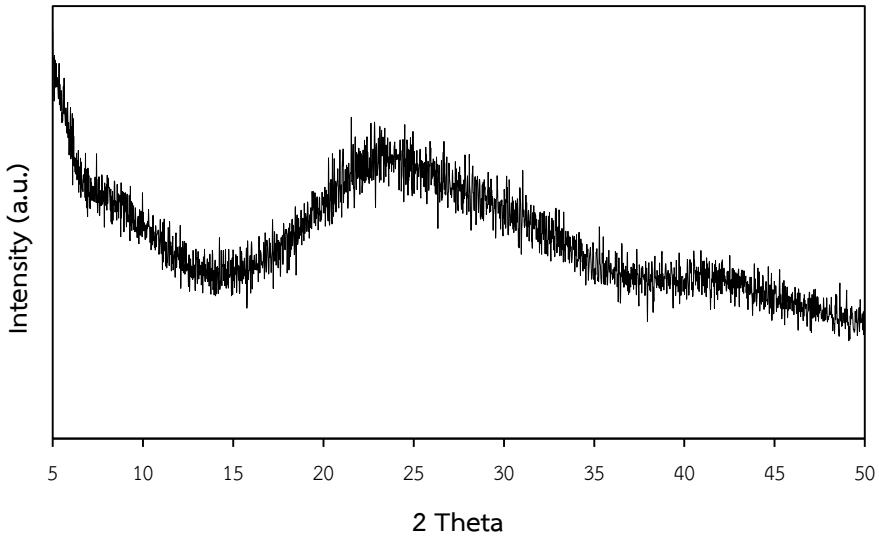

Fig. 4.3 XRD pattern of electrospun silica fiber.

4.1.2 The properties of commercial silica (porous)

The Fuji Silysia SiO_2 (5-10 mesh) or commercial silica (porous) was used as the catalyst support. Due to porous properties, it contains surface area 237.36 m^2/g and pore volume 1.010 cm^3/g that higher than electrospun silica fiber. The pore size of this support is 16.900 Å. The morphology and the particle size are determined by SEM image with magnification 30 that shown in Fig. 4.4 (a). The result indicated that commercial silica (porous) has irregular shape with the particle size 511.59 μm. Fig 4.4 (b) shows the SEM image of commercial silica (porous) with magnification 1000 indicating that it has rough surface. The XRD pattern in Fig. 4.5 exhibits the amorphous silica pattern similar with electrospun silica fiber.

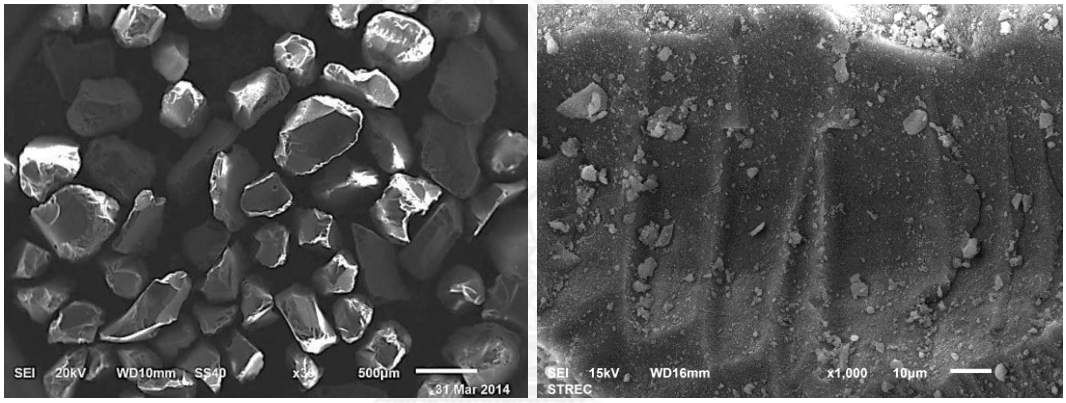

Fig. 4.4 SEM images of commercial silica (porous) with magnification (a) 30 (b) 1000

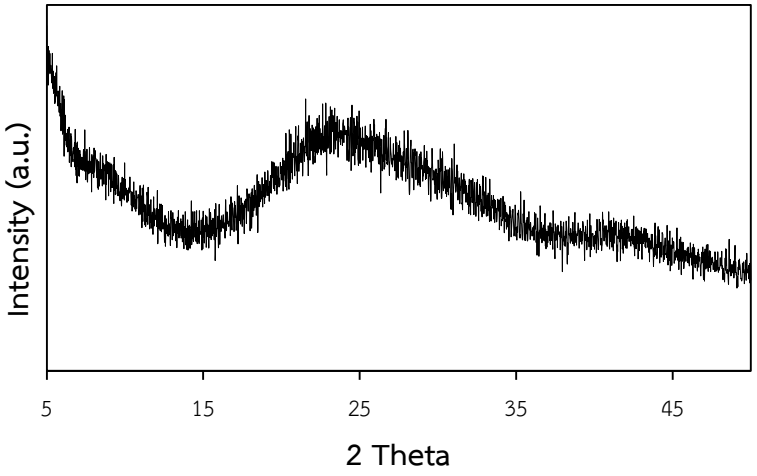

Fig. 4.5 XRD pattern of commercial silica (porous).

4.1.3 The properties of ZSM-5 on electrospun silica fiber with Si/Al 20

ZSM-5 on electrospun silica fiber with Si/Al 20 was prepared under pH 9, hydrothermal time 24 h. and hydrothermal temperature 180 °C. The BET surface area and pore volume was 70.74 m^2/g and 0.051 cm^3/g respectively that higher than bare electrospun silica fiber due to porosity of ZSM-5. The ZSM-5 deposition on electrospun silica fiber was shown in Fig. 4.6. The small crystals deposited on fiber with crystal size 1.76 μm. The crystalline structure was confirmed by XRD pattern in Fig. 4.7 that compose of two characteristic peaks at 2 theta between 7-10 and 22-25 corresponding to the MFI structure [42, 45]

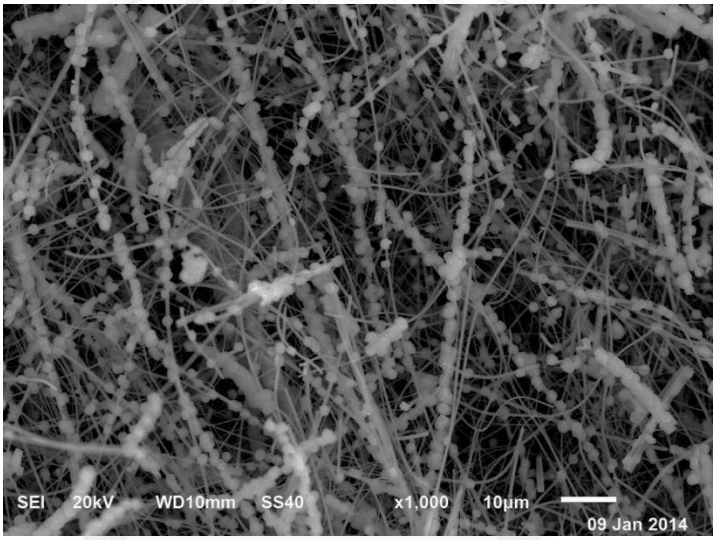

Fig. 4.6 SEM image of ZSM-5 on electrospun silica fiber with Si/Al 20.

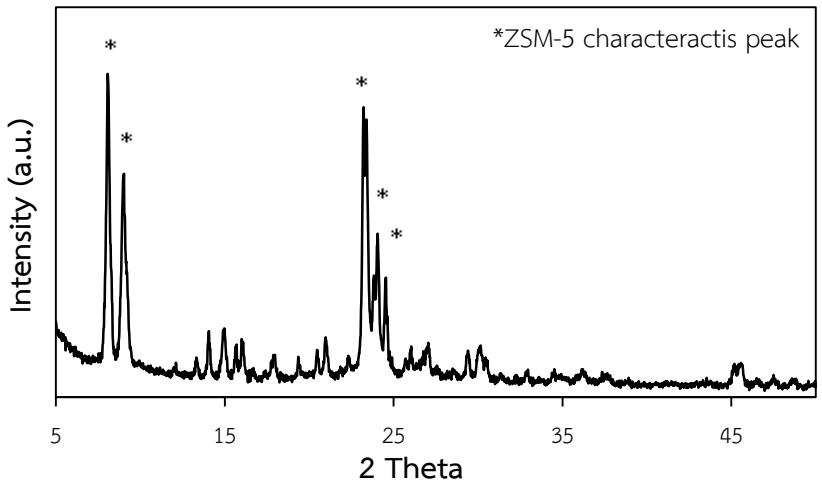

Fig. 4.7 XRD pattern of ZSM-5 on electrospun silica fiber with Si/Al 20.

4.1.4 The properties of commercial ZSM-5 (porous)

The NH_3-ZSM-5 with the name HSZ-800 (840NHA) is aluminosilicate zeolite that composes of Si/Al ratio 20. It can convert to H-ZSM-5 by calcination at 550 °C for 5 h prior using. The crystal appearance was presented in Fig. 4.8, the agglomeration of hexagonal shape was found with average crystal size 3.58 μm. The crystalline structure of commercial ZSM-5 was confirmed by XRD pattern in Fig. 4.9. The physical properties including surface area, total pore volume, pore diameter and average particle size are summarized in table 4.1. Commercial ZSM-5 exhibited higher surface area comparing with silica fiber, commercial silica (porous) and ZSM-5 on electrospun silica fiber with Si/Al 20.

Table 4.1 Properties of commercial ZSM-5 with the name HSZ-800 (840NHA)

Properties	**HSZ-800 (840NHA)**
Si/Al	20
Surface area (BET, m^2/g)	433.80
Total pore volume (cm^3/g)	0.225
Pore diameter (Å)	20.690
Crystal size (μm) [a]	3.58

[a]Measured by SEM

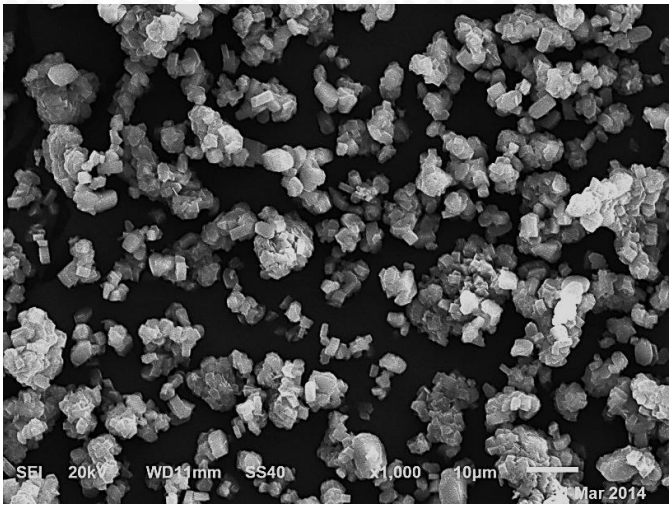

Fig. 4.8 SEM image of commercial ZSM-5 with Si/Al 20.

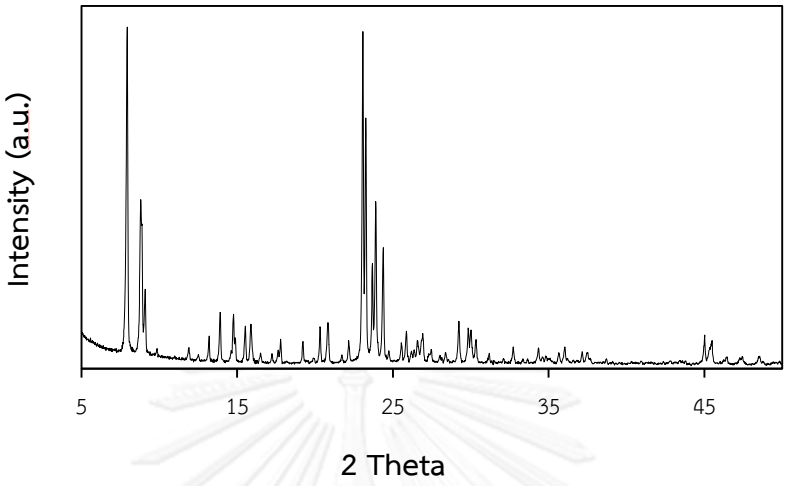

Fig. 4.9 XRD pattern of commercial ZSM-5 with Si/Al 20.

4.2 ZSM-5 synthesized on electrospun silica fiber

4.2.1 The effect of pH

The influence of pH solution for ZSM-5 synthesis on electrospun silica fiber has been studied by varying pH from 8 to 10 with the condition of Si/Al 40 and hydrothermal performed at 180 °C for 24 hours. Increasing of pH leads to supersaturated of silicate and aluminate species, more nuclei are formed [11] resulting in smaller crystal size and more crystal growth on the fiber as shown in Fig. 4.10. The synthesized ZSM-5 with pH 8 9 and 10 have crystal size decreasing from 2.32 μm to 1.63 μm. The XRD patterns in Fig. 4.11 indicate that all synthesized samples display the MFI structure and intensity of signal tends to increase with increase pH. The higher BET surface area and pore volume was found that illustrated in table 4.2. The pore size of fibrous form ZSM-5 was not determined because it had inter-fiber void space which is random value. Although synthesizing under high pH yielded more ZSM-5 deposition but the dissolution of electrospun silica also increased especially at pH 10 [50] thus preparing at pH 9 is the optimum condition for preparation of ZSM-5 on silica fiber.

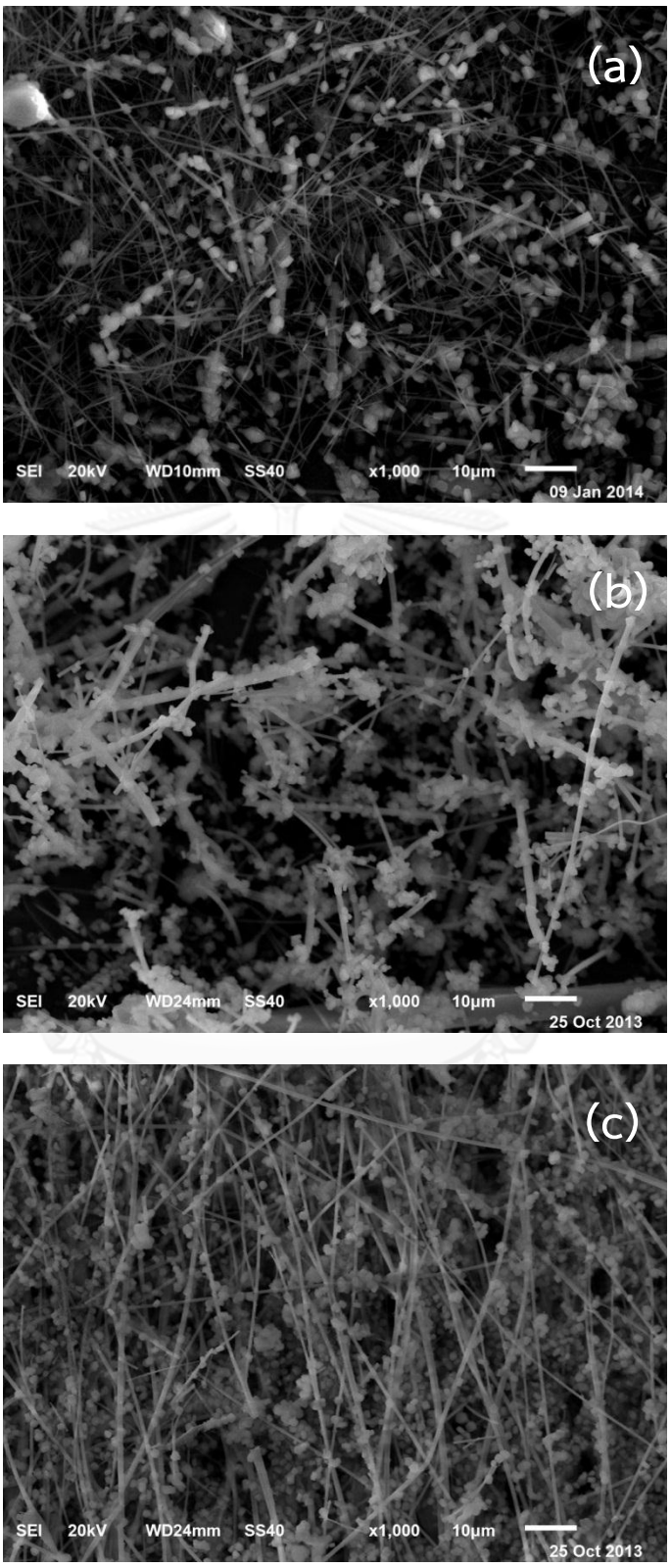

Fig. 4.10 SEM images of ZSM-5 on electrospun silica fiber synthesized at (a) pH 8 (b) pH 9 and (c) pH 10.

Table 4.2 Crystal size, BET surface area, pore size and pore volume of ZSM-5 on electrospun silica fiber synthesized at pH 8 to 10.

pH	Crystal size (μm) [a]	Surface area (BET, m^2/g)	Pore size (Å)	Pore volume (cm^3/g)
8	2.32	70.58	43.460	0.077
9	1.87	189.04	24.806	0.117
10	1.63	194.30	26.094	0.127

[a] Measured by SEM.

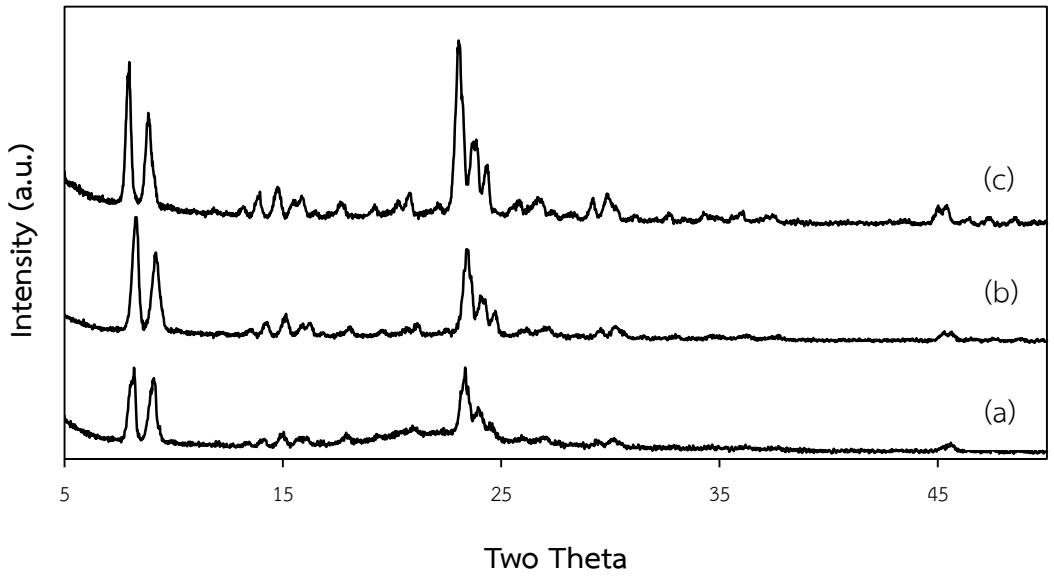

Fig 4.11 XRD patterns of ZSM-5 on electrospun silica fiber with synthesized at (a) pH 8 (b) pH 9 and (c) pH 10.

4.2.2 The effect of hydrothermal temperature

The morphology of ZSM-5 on electrospun silica fiber preparing with hydrothermal temperature from 170 to 190 °C is presented in Fig. 4.12. At higher temperature, the nucleation rate and crystal growth rate were promoted [10, 51] however synthesizing at 190 °C is not appropriate attribute to the excessive ZSM- 5

growth on the fibrous support resulting in the brittle fiber. At 180 °C, the ZSM-5 crystals were orderly deposited on fiber whereas synthesizing at 170 °C presented the agglomeration of ZSM-5 crystals due to competitive parameters between rate of ZSM-5 formation on the fiber and leaching of silica seed gel from fiber. Synthesizing at 180 °C, ZSM-5 crystals rapidly formed at silica seed gel on the fiber resulting in low leaching of silica seed gel from the fiber therefore the crystals arranged orderly. In contrast, crystals formation on fiber was slow at 170 °C and silica seed gel on fiber was leached from fiber with increasing time therefore ZSM-5 crystals were grown in some position resulting in agglomeration of crystals. XRD patterns in Fig. 4.13 show the characteristic peak of ZSM-5 and similar intensity. The crystal size, surface area, pore size and pore volume are illustrated in table 4.3. The crystal size is ranging between 1.74 to 2.70 μm and tends to increase with increasing of temperature resulting from acceleration of crystal growth [52]. The BET surface area of ZSM-5 synthesizing at 170 °C was larger than 180 °C attribute to leaching of silica seed gel from the fiber and inducing of ZSM-5 formation in the solution [53, 54]. Therefore re-deposition of ZSM-5 crystals on the fiber also increased. Although synthesizing at 180 °C yielded lower surface area than 170 °C but it had orderly arrangement on fiber. Therefore synthesizing at 180 °C is the most appropriate condition.

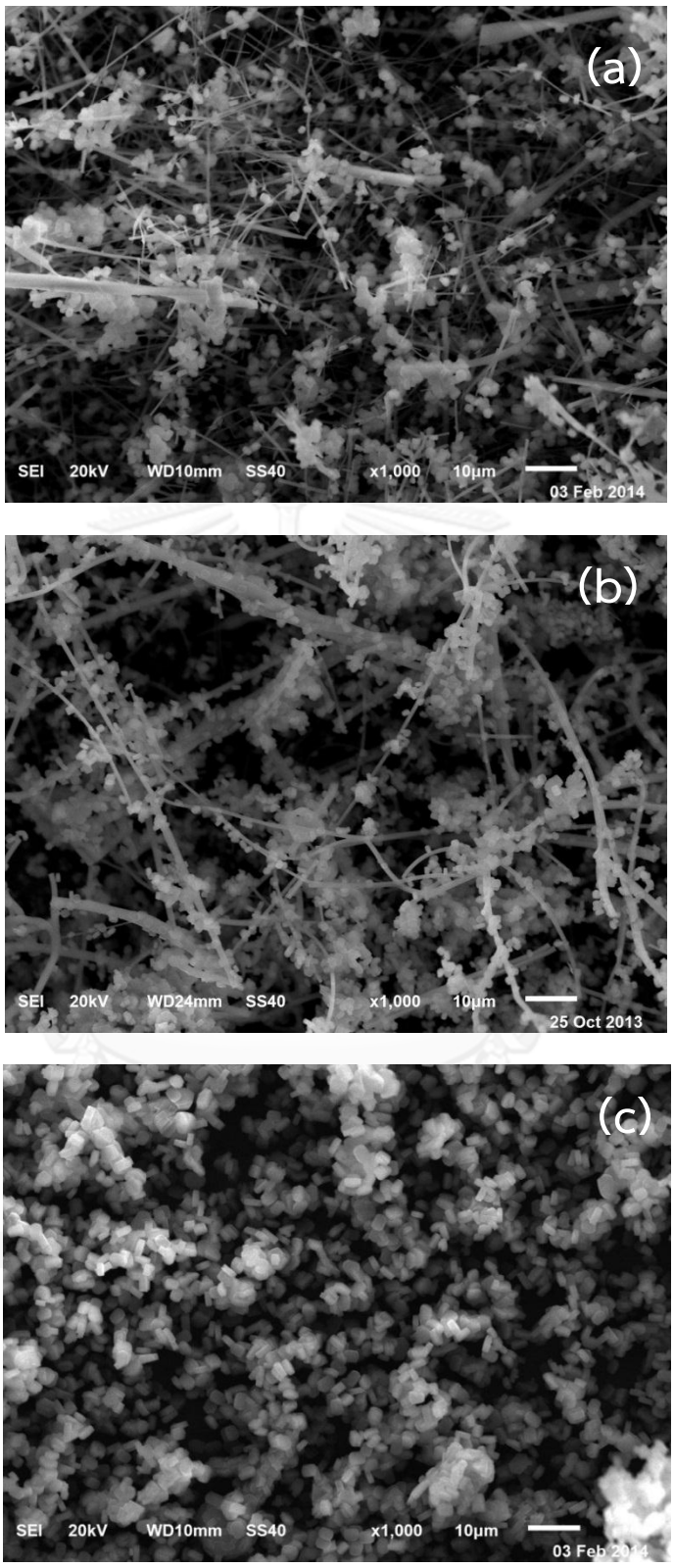

Fig. 4.12 SEM images of ZSM-5 on electrospun silica fiber synthesized at (a) 170 °C (b) 180 °C and (c) 190 °C.

Table 4.3 Crystal size, BET surface area, pore size and pore volume of ZSM-5 on electrospun silica fiber synthesized at 170 to 190 °C.

Temperature (°C)	Crystal size (μm) [a]	Surface area (BET, m^2/g)	Pore size (Å)	Pore volume (cm^3/g)
170	1.85	230.42	25.502	0.147
180	1.87	189.04	24.806	0.117
190	2.70	294.51	24.688	0.182

[a] Measured by SEM.

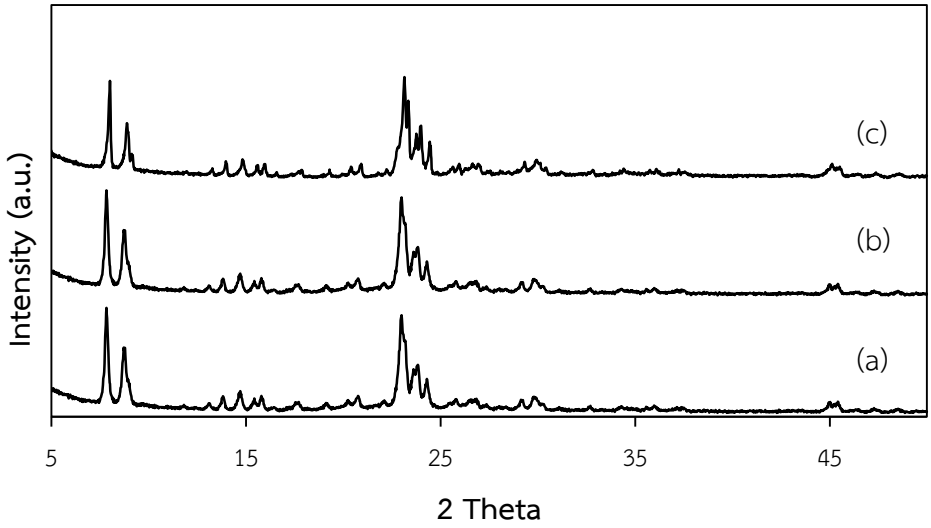

Fig. 4.13 XRD patterns of ZSM-5 on electrospun silica fiber synthesized at (a) 170 °C (b) 180 °C and (c) 190 °C.

4.2.3 The effect of hydrothermal time

The influence of hydrothermal time for ZSM-5 coating has been investigated at 24, 48, 60 and 72 h. The SEM image in Fig. 4.14 presents the plenty of ZSM-5 deposition with increase the hydrothermal time and the crystal size become larger from 1.72 to 3.22 μm. Fig. 4.14 (a) shows the regular dispersion of ZSM-5 crystals on fiber thus using 24 h of hydrothermal time is the most suitable. The

XRD patterns in Fig 4.15 indicate the higher intensity with increasing hydrothermal time that is correspondingly with the SEM images.

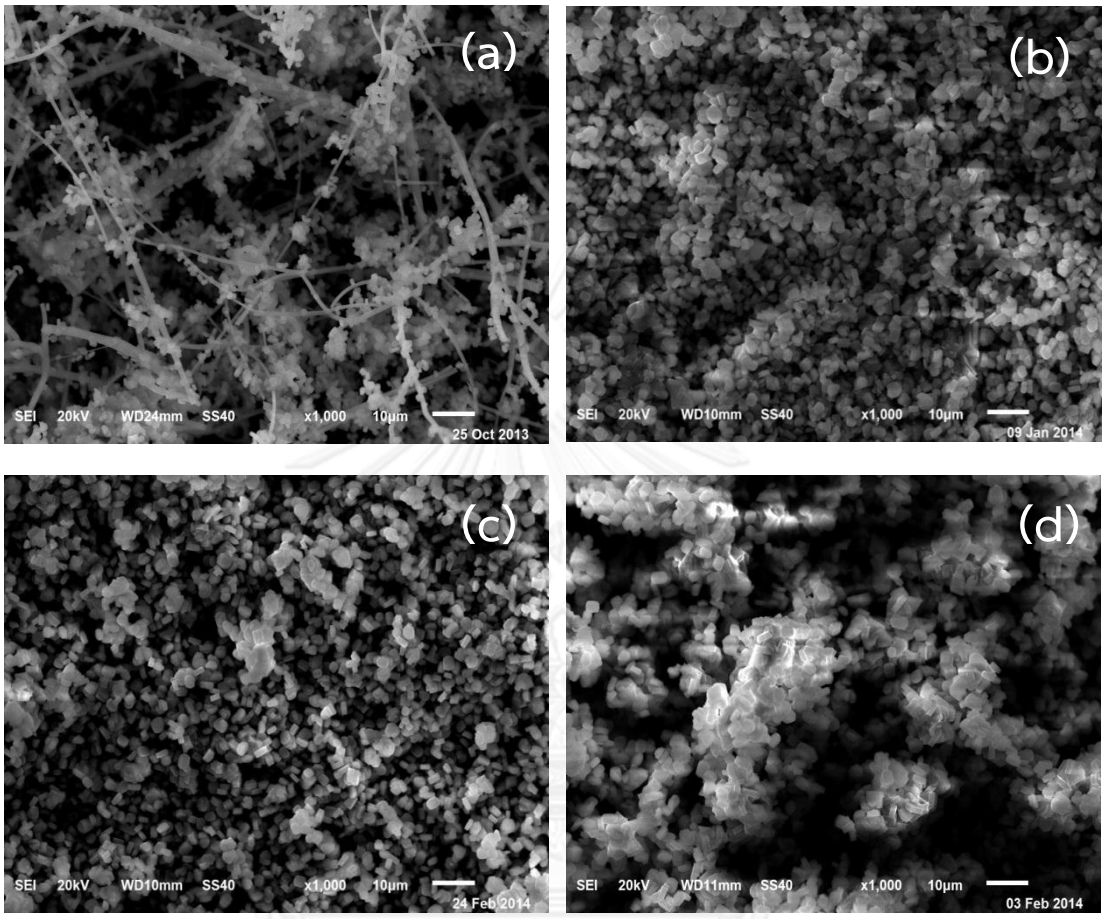

Fig. 4.14 SEM images of ZSM-5 on electrospun silica fiber synthesized with hydrothermal time (a) 24 h (b) 48 h (c) 60 h and (d) 72 h.

Table 4.4 Crystal size, BET surface area, pore size and pore volume of ZSM-5 on electrospun silica fiber synthesized with hydrothermal time 18 to 72 h.

Time (h)	Crystal size (μm) [a]	Surface area (BET, m^2/g)	Pore size (Å)	Pore volume (cm^3/g)
24	1.87	189.04	24.806	0.117
48	2.58	322.02	25.273	0.172
60	2.67	326.45	25.048	0.204
72	3.22	436.80	20.69	0.225

[a] Measured by SEM.

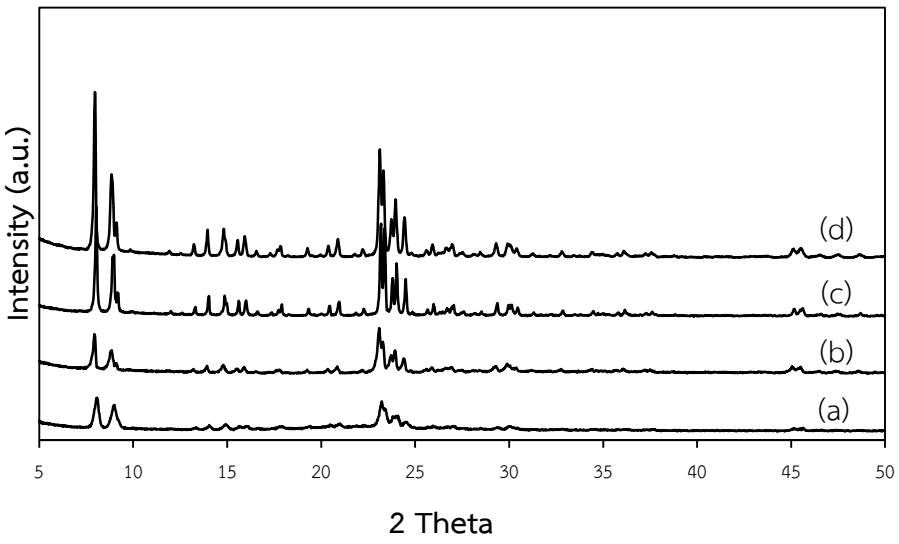

Fig. 4.15 XRD patterns of ZSM-5 on electrospun silica fiber synthesized with hydrothermal time (a) 24 h (b) 48h (c) 60 h (d) 72 h.

4.2.4 The effect of Si/Al ratio

Fig. 4.16 shows the SEM images of ZSM-5 on electrospun silica fiber at Si/Al ratios 20, 40, 60 and 80 preparing with pH 9 and using hydrothermal condition 180 °C for 24 h. The high deposition of ZSM-5 on electrspun silica fiber was found with increasing of Si/Al ratio. As Si rich solution, the silicate species were induced by template (TPAOH) resulting in super-saturation, lowering induction period therefore rate of nucleation and rate of crystallization were increased [55]. The crystal sizes of ZSM-5

with Si/Al 20 to 80 were shown in table 4.5, the average crystal sizes increased as Si/Al ratio increased and the crystal sizes were ranging from 1.74 to 2.34 μm corresponding with the research of Shirazi, L. [56] and Lin, J.C. [57]. BET surface area in table 4.5 indicated that high Si/Al ratios lead to increase surface area [58] resulting from enhancing of ZSM-5 deposition on fiber. ZSM-5 with Si/Al 20 exhibits the lowest surface area with 70.74 m^2/g and the highest is Si/Al 80 with surface area 277.80 m^2/g. The crystal growth of ZSM-5 with Si/Al 40 and 60 were similar but Si/Al 40 generated little higher surface area due to smaller crystal. The increasing of pore volume at high Si/Al indicated the higher porosity. Thickness of ZSM-5 deposition is illustrated in table 4.6 that was measured by comparing with bare electrospun silica, an enlargement of thickness from 1.00 to 1.52 μm was found with increasing Si/Al ratio from 20 to 80 due to larger ZSM-5 crystal size and higher crystal deposition. XRD patterns of ZSM-5 with Si/Al ratios 20 to 80 are shown in Fig. 4.17. The XRD peak intensity increased with the increase of Si/Al ratios corresponding with SEM images.

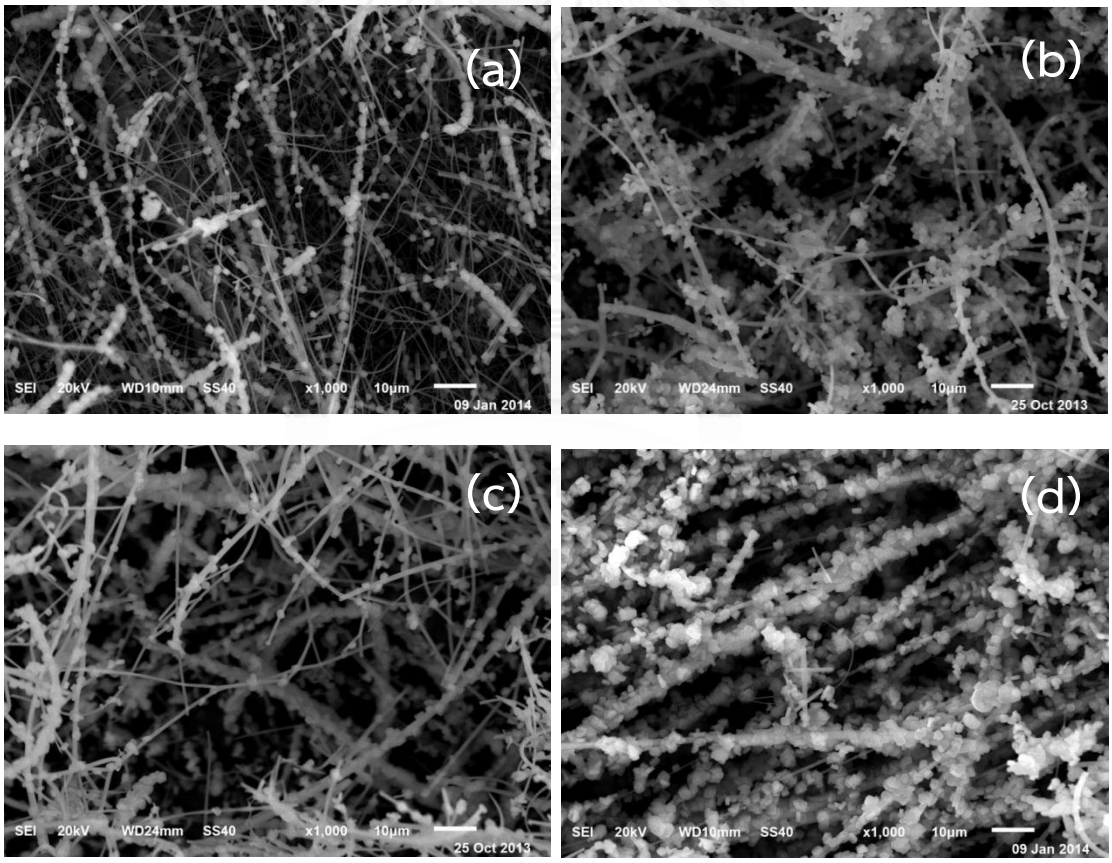

Fig. 4.16 SEM images of ZSM-5 on electrospun silica fiber with Si/Al (a) 20 (b) 40 (c) 60 and (d) 80.

Table 4.5 Crystal size, BET surface area, pore size, pore volume, diameter of ZSM-5 deposition on fiber and thickness of ZSM-5 deposition on electrospun silica fiber with Si/Al 20 to 80.

Si/Al	Crystal size (μm) [a]	Surface area (BET, m^2/g)	Pore size (Å)	Pore volume (cm^3/g)	Diameter of ZSM-5 deposition on fiber (μm)	Thickness of ZSM-5 deposition (μm) [b]
20	1.76	70.74	29.09	0.051	2.67	1.00
40	1.87	189.04	24.80	0.117	2.84	1.08
60	2.23	188.50	33.49	0.157	3.32	1.32
80	2.34	277.80	27.91	0.193	3.71	1.52

[a] Measured by SEM.

[b] Thickness = (Diameter of ZSM-5 deposited on fiber – diameter of electrospun silica fiber) ÷ 2 where diameter of electrospun silica fiber = 0.68 μm.

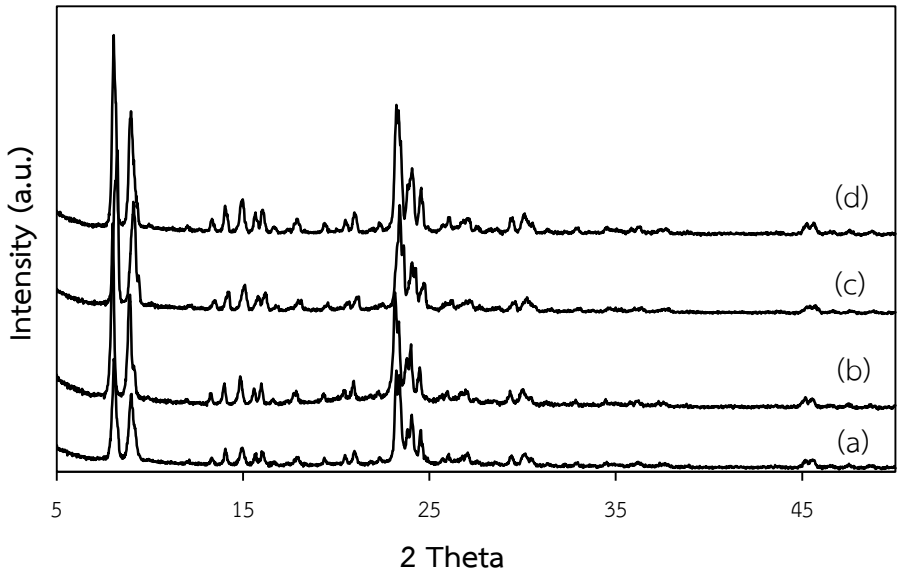

Fig. 4.17 XRD patterns of ZSM-5 on electrospun silica fiber with Si/Al (a) 20 (b) 40 (c) 60 and (d) 80.

4.3 Catalyst characterization

The previous section can conclude that synthesizing under pH 9 with hydrothermal condition 180 °C for 24 h. showed the good dispersion of ZSM-5 on electrospun silica fiber and the properties of fiber were maintained. The increase of Si/Al ratio also increased coating thickness but its Al content played important role to the catalytic properties thus it should be considered in the next step. In this section, CO hydrogenation reaction was used to study the catalytic performance. The catalysts were prepared by loading 10 % Co onto fiber and porous support including ZSM-5 on electrospun silica fiber with various Si/Al ratios (20 to 80). All prepared catalysts were characterized with EDX to measure element components and using XRD to study crystalline structure and crystal size of cobalt catalyst then studied the reduction behavior by temperature reduction program (TPR)

4.3.1 Catalyst characterization by SEM

Fig. 4.18 is the SEM images with magnification 20,000 times of electrospun silica fiber, commercial silica (porous), commercial ZSM-5 (porous) and ZSM-5 on electrospun silica fiber (Si/Al ratio 20, 40, 60 and 80) loading with 10%wt of cobalt. These catalysts were given in the name 10Co_electrospun silica fiber, 10Co_commercial silica (porous), 10Co_commercial ZSM-5 (porous), 10Co_ZSM-5_Si/Al 20 fiber, 10Co_ZSM-5_Si/Al 40 fiber, 10Co_ZSM-5_Si/Al 60 fiber and 10Co_ZSM-5_Si/Al 80 fiber. Due to nonporous properties of electrospun silica fiber, the cobalt particles mostly disperse on the fiber surface as illustrated Fig. 4.18 (a) which can observe as small dots. In contrary, the cobalt dispersion on porous material (Fig. 4.18 (b) to (g)) is not clearly seen probably due to penetration of cobalt into the pores.

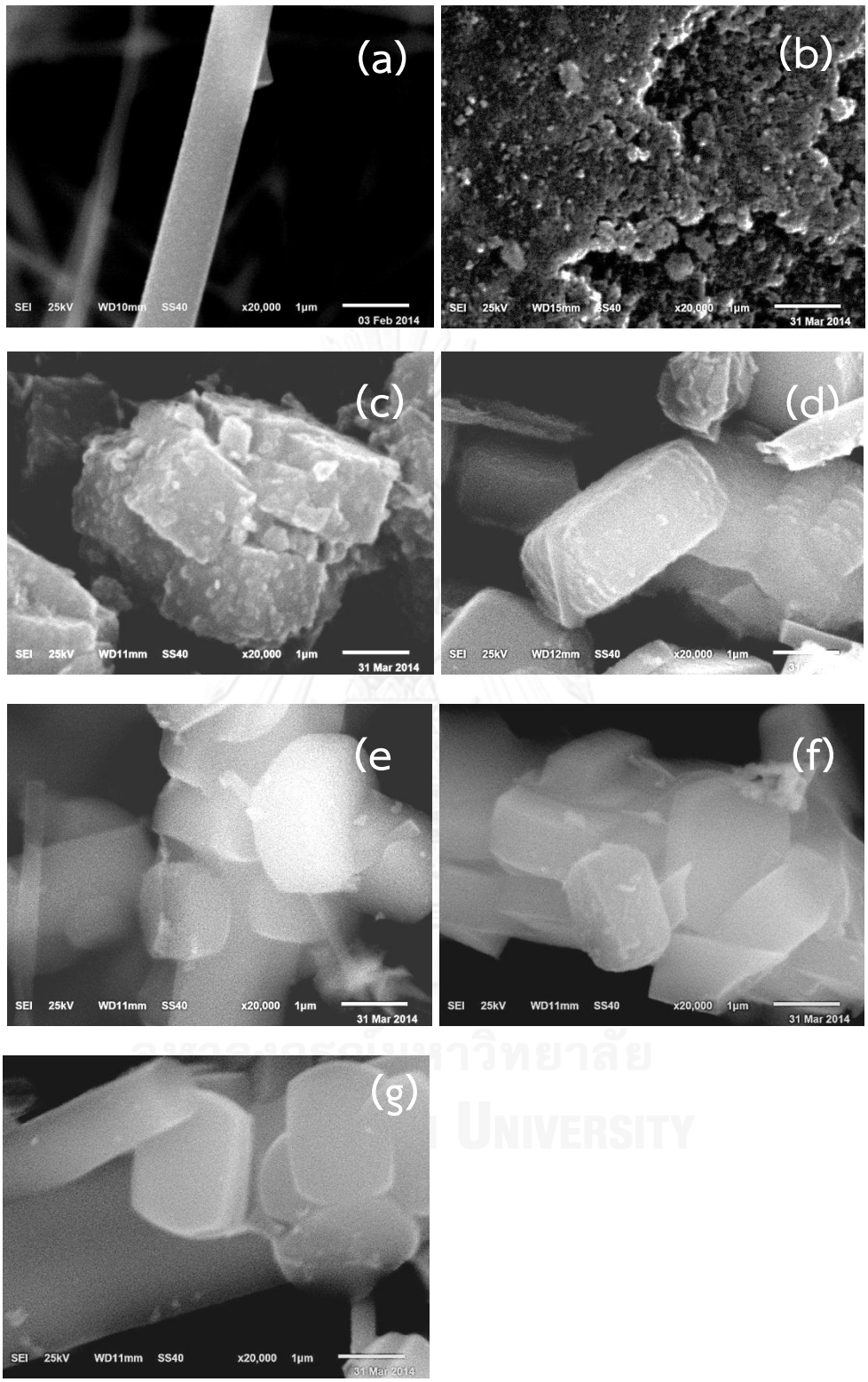

Fig. 4.18 SEM images of fiber and porous catalysts (a) 10Co_electrospun silica fiber (b) 10Co_commercial silica (porous) (c) 10Co_commercial ZSM-5 (porous) (d) 10Co_ZSM-5_Si/Al 20 fiber (e) 10Co_ZSM-5_Si/Al 40 fiber (f) 10Co_ZSM-5_Si/Al 60 fiber and (g) 10Co_ZSM-5_Si/Al 80 fiber.

4.3.2 Catalyst characterization by EDX

The components of these catalysts were measured by EDX technique as illustrated in table 4.6. The results showed that the electrospun silica fiber and commercial silica (porous) composed of Si and O whereas ZSM-5 porous and fiber support contained Si, Al and O. The Si/Al ratios (EDX) of ZSM-5 on electrospun silica are higher than the calculation due to background interference of electrospun silica fiber. The cobalt content was detected ranging from 6.68 to 11.56% by weight which confirmed the SEM images that there is cobalt dispersion on the silica and ZSM-5 support.

Table 4.6 Components of Si, Al, and Co in the fiber and porous catalysts measured by EDX**.**

Type of catalyst	Co (% wt.)	Si/Al [a]	Si/Al [b]	Si (% atom)	Al (% atom)	O (% atom)
10Co_electrospun silica fiber	10.90	-	-	24.56	-	71.61
10Co_commercial silica (porous)	9.07	-	-	31.57	-	65.16
10Co_commercial ZSM-5 (porous)	10.30	20	14.90	20.70	1.40	74.38
10Co_ZSM-5_Si/Al 20 fiber	6.68	20	36.35	25.08	0.69	71.95
10Co_ZSM-5_Si/Al 40 fiber	6.94	40	70.79	26.90	0.38	70.32
10Co_ZSM-5_Si/Al 60 fiber	9.45	60	82.63	47.10	0.57	48.59
10Co_ZSM-5_Si/Al 80 fiber	11.56	80	81.76	41.77	0.51	53.2

[b] Si/Al from calculation.

[b] Si/Al from EDX.

4.3.3 Catalyst characterization by XRD

The XRD patterns in Fig. 4.19 confirmed the crystal structure of Co_3O_4 that located at 2 theta = 18, 31, 37, 45, 59 and 65 [59, 60]. The Co_3O_4 and Co crystal sizes were measured by XRD that presented in table 4.6. In case of electrospun silica fiber, the crystal size of cobalt species was larger than other types of support. Due to its small surface area, therefore cobalt dispersion was poor resulting in the large crystal size [61]. The commercial ZSM-5 (porous) had smaller cobalt crystal size comparing with commercial silica (porous) due to two factors which are surface area and Al content in the framework. Commercial ZSM-5 contained surface area 433.80 m^2/g whereas commercial silica (porous) was 237.36 m^2/g therefore cobalt dispersion in the first support was greater and led to smaller cobalt crystal size. Furthermore, addition of aluminium into the framework created more acid site that had strong interaction between the support and cobalt species leading to small crystal size of cobalt. The increasing of Si/Al ratios from 20 to 80 affected to increase cobalt particle size due to weak cobalt-support interaction.

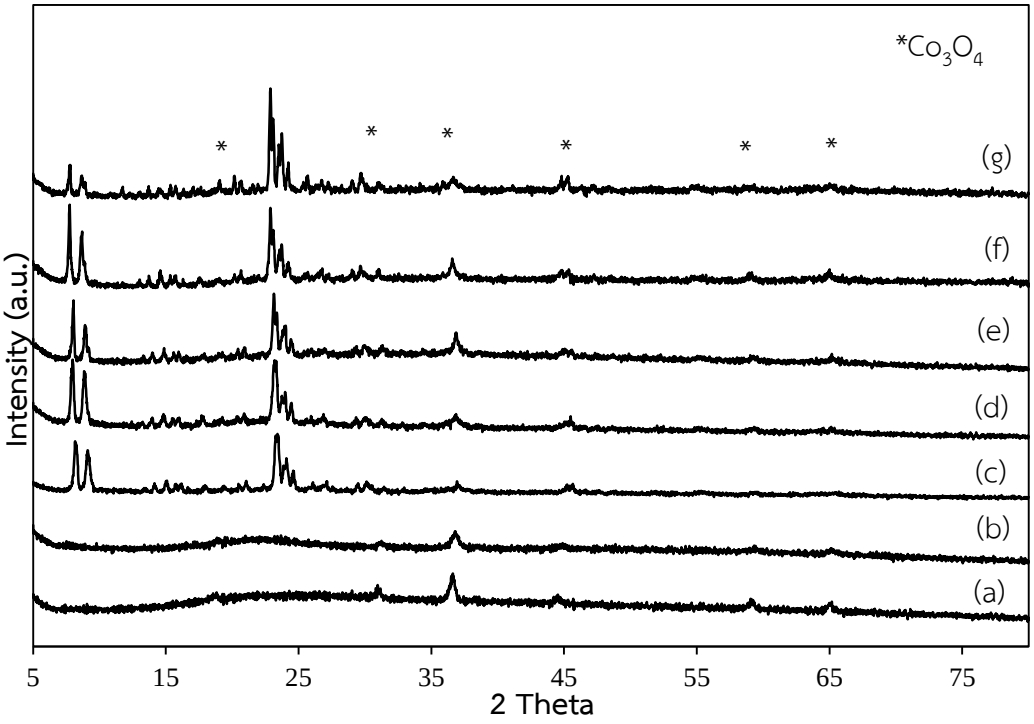

Fig. 4.19 XRD patterns of fiber and porous catalyst (a) 10Co_electrospun silica fiber (b) 10Co_commercial silica (porous) (c) 10Co_ZSM-5_Si/Al 20 fiber (d) 10Co_ZSM-5_Si/Al 40 fiber (e) 10Co_ZSM-5_Si/Al 60 fiber (f) 10Co_ZSM-5_Si/Al 80 fiber and (g) commercial ZSM-5 (porous).

Table 4.7 Crystal size of Co_3O_4 and Co on fiber and porous catalyst measured by XRD

Type of catalyst	Co_3O_4 crystal size (nm)	Co crystal size* (nm)
10Co_electrospun silica fiber	27.17	20.38
10Co_commercial silica (porous)	17.92	13.44
10Co_commercial ZSM-5 (porous)	12.82	9.62
10Co_ZSM-5_Si/Al 20 fiber	16.96	12.72
10Co_ZSM-5_Si/Al 40 fiber	21.27	15.95
10Co_ZSM-5_Si/Al 60 fiber	22.27	16.70
10Co_ZSM-5_Si/Al 80 fiber	23.20	17.40

*$d(Co^0) = 0.75 \times d(Co_3O_4)$ [38]

4.3.4 Catalyst characterization by TPR

TPR profiles of fiber and porous catalyst are shown in Fig. 4.20. The region between 300 to 500 °C demonstrated the reducibility of $Co_3O_4 \rightarrow CoO \rightarrow Co^0$ [39]. The first peak at low temperature assigned to the reduction of Co_3O_4 to CoO presenting in small shoulder peak. The second peak at higher temperature indicated the reduction of CoO to Co^0. Moreover, the broad peak in the reduction of CoO to Co^0 was found in SiO_2 porous and commercial ZSM-5 porous due to stepwise reduction of various Co^{2+} species or reduction inside the pore. The third reduction peak higher than 650 °C was found in 10Co_SiO_2 porous and 10Co_commercial ZSM-5 (porous) attributed to less reducible of cobalt species like cobalt silicates or cobalt aluminates phase [31]. The fibrous form catalysts completely reduced approximate to 500 °C which lower than porous catalysts. Table 4.8 indicated the % reduction of porous and fiber catalyst which are ranging from 43.50 to 73.18. The porous catalyst gave the lower % of reduction comparing with fibrous form catalyst due to the partly penetration of Co_3O_4 to inner pores leading to lower reducibility. Increasing of Si/Al ratio resulted in improving the % of reduction due to weaker interaction between

cobalt catalysts and Al in the support. Therefore the reducibility can be improved by using fibrous catalyst and increasing of Si/Al ratio.

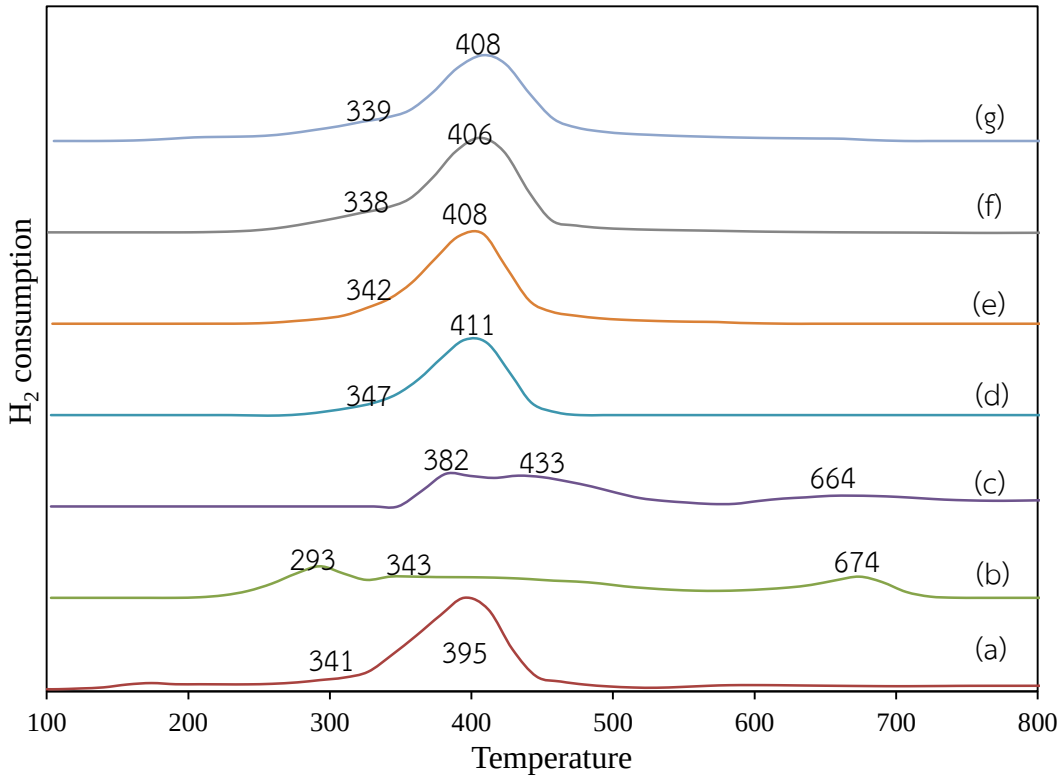

Fig. 4.20 TPR profile of fiber and porous catalysts (a) 10Co_electrospun silica fiber (b) 10Co_commercial silica (porous) (C) 10Co_commercial ZSM-5 (porous) (d) 10Co_ZSM-5_Si/Al 20 fiber (e) 10Co_ZSM-5_Si/Al 40 fiber (f) 10Co_ZSM-5_Si/Al 60 fiber and (g) 10Co_ZSM-5_Si/Al 80 fiber.

Table 4.8 Reduction temperature and % reduction of fiber and porous catalysts measured by TPR

Type of catalyst	Reduction temperature (°C)			% Reduction
	1st	2nd	3rd	
10Co_electrospun silica fiber	341	395	-	73.18
10Co_commercial silica (porous)	293	343	674	56.86
10Co_commercial ZSM-5 (porous)	382	433	664	47.50
10Co_ZSM-5_Si/Al 20 fiber	347	411	-	61.51
10Co_ZSM-5_Si/Al 40 fiber	342	408	-	62.06
10Co_ZSM-5_Si/Al 60 fiber	338	406	-	66.60
10Co_ZSM-5_Si/Al 80 fiber	339	408	-	72.51

4.4 Catalytic testing by CO hydrogenation reaction

4.4.1 The effect of Si/Al ratios to catalytic activity

Fig. 4.21 shows the CO conversion of 10Co_ZSM-5 fiber with Si/Al 20 to 80. The lowest CO conversion was found in 10Co_ZSM-5_Si/Al 20 fiber and tended to increase at higher Si/Al ratios. Table 4.9 presents %CO conversion of Si/Al 20, 40, 60 and 80 which are 34.29, 36.08, 37.01 and 42.99 %, respectively. These results are related with cobalt crystal size and surface area of support [61]. High Si/Al ratio leads to weak metal-support interaction and the large cobalt crytal sizes that prevents re-oxidized to inactive cobalt species therefore the higher CO conversion was found [62]. The large surface area of support allows a high degree of cobalt dispersion and reactants are easy to contact with active site leading to high CO conversion [61, 63].

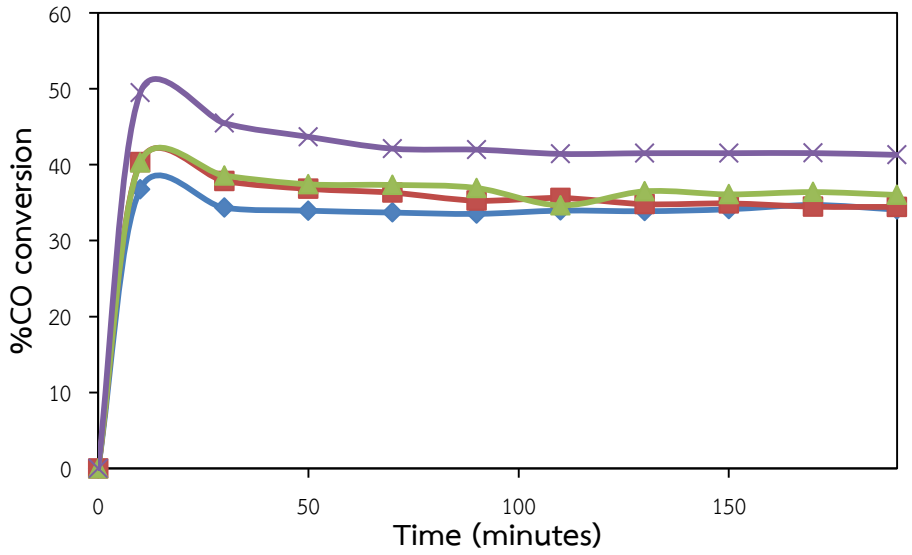

Fig. 4.21 %CO conversion of (♦) 10Co_ZSM-5_Si/Al 20 fiber (■) 10Co_ZSM-5_Si/Al 40 fiber (▲) 10Co_ZSM-5_Si/Al 60 fiber and (×) 10Co_ZSM-5_Si/Al 80 fiber with reaction time 0 to 190 minutes.

4.4.2 The effect of Si/Al ratios to product selectivity

Fig. 4.22 shows product selectivity of CO hydrogenation reaction with the catalysts 10Co_ZSM-5 fiber (Si/Al 20 to 80). The major product from this process is CH_4 and the minor products are C_2H_4 and CO_2. Selectivity of CH_4 with Si/Al 20, 40, 60 and 80 is reported Table 4.9 which are 93.10, 92.79, 88.68 and 88.33 %, respectively. Decreasing Si/Al ratio leads to higher CH_4 selectivity [40, 61, 63]. This is associated with strong metal-support interaction and the decrease in cobalt crystal size that affects a lower coverage of CO and a larger coverage of H_2 [41]. Therefore, CH_4 selectivity is improved by decreasing Si/Al ratio and cobalt crystal size. CO_2 selectivity tends to increase with increasing Si/Al ratio due to high coverage of CO and increasing in CO conversion into products including water which is the precursor for water gas shift reaction leading to increase selectivity CO_2 and inhibits CH_4 formation.

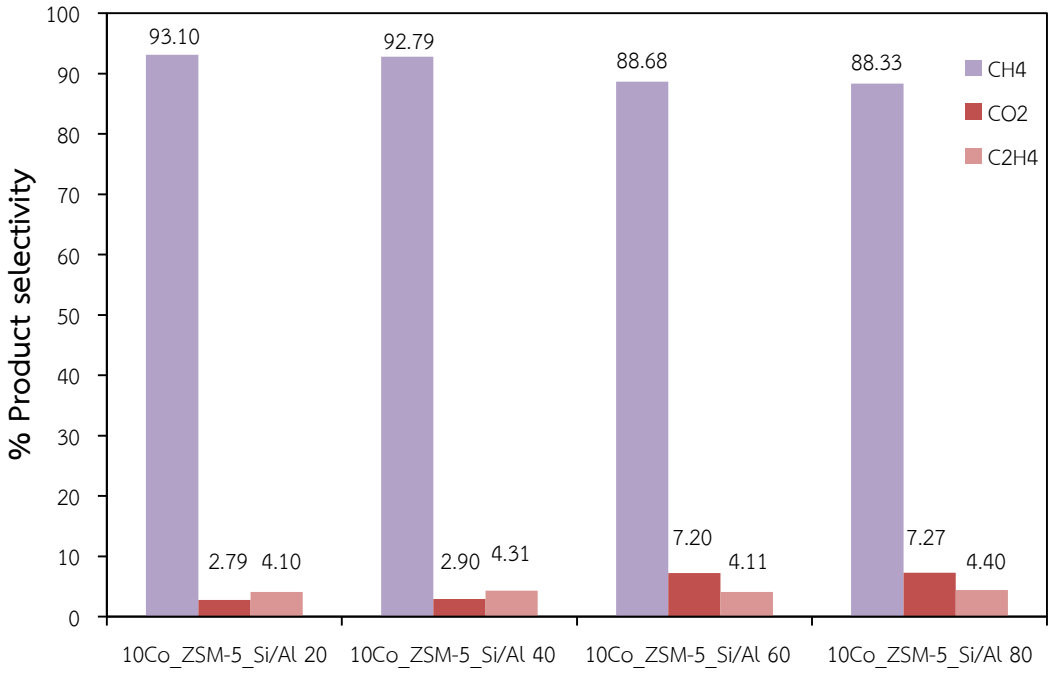

Fig. 4.22 %Product selectivity of 10Co_ZSM-5_Si/Al 20 fiber, 10Co_ZSM-5_Si/Al 40 fiber, 10Co_ZSM-5_Si/Al 60 fiber and 10Co_ZSM-5_Si/Al 80 fiber with reaction time 0 to 190 minutes.

4.4.3 The effect of support to catalytic activity

The commercial silica (porous) generates higher CO conversion than electrospun silica fiber due to its large surface area as and high metal dispersion. Fig. 4.23 indicated that the commercial silica (porous) is less stability than fiber due to large particle size (long diffusion path length) therefore mass and heat transfer are poor and the catalyst deactivates easily. At first 170 minutes, the commercial silica (porous) exhibited high CO conversion with 94.57- 98.89% after that CO conversion decreased to 73.40% whereas electrospun silica fiber gave more stability, the CO conversion began to smooth after 30 minute. In case of SiO_2 porous and commercial ZSM-5 (porous), commercial ZSM-5 (porous) showed a lower CO conversion due to smaller cobalt crystal size and the strong metal-support interaction in ZSM-5. Commercial ZSM-5 (porous) has higher CO conversion than 10Co_ZSM-5_Si/Al 20 due to larger cobalt crystal size and larger surface area whereas the stability is similar.

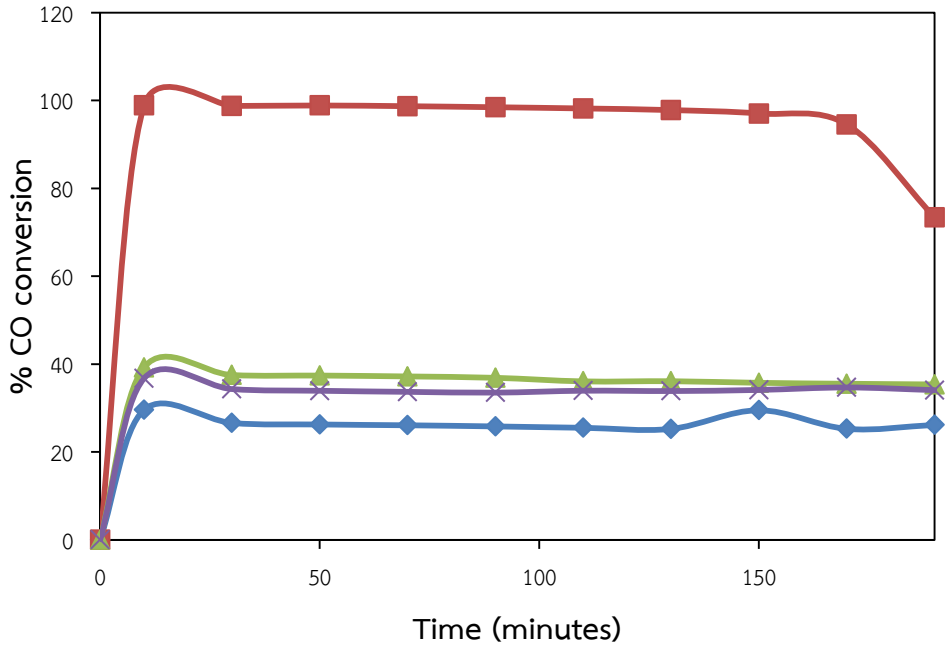

Fig. 4.23 %CO conversion of (♦) 10Co_electrospun silica fiber (■) 10Co_commercial silica (porous) (▲) 10Co_commercial ZSM-5 (porous) and (×) 10Co_ZSM-5_Si/Al 20 with reaction time 0 to 190 minutes.

4.4.4 The effect of support to product selectivity

Fig 4.24 illustrated product selectivity of different supported catalyst which is 10Co_electrospun silica fiber, 10Co_ commercial silica (porous), 10Co_commercial ZSM-5 (porous) and 10Co_ZSM-5_Si/Al 20. The results indicated that 10Co_commercial silica (porous) yielded lower CH_4 selectivity than 10Co_electrospun silica fiber and the fibrous form of 10Co_ZSM-5_Si/Al 20 because the commercial silica (porous) contains high CO conversion and generates high water content including long diffusion path length therefore the catalyst can adsorb large amount of water inside the pore and react with CO to yield H_2 and CO_2 as shown in equations 4.1 and 4.2

CO hydrogenation reaction: $(2n+1)\ H_2 + nCO \rightarrow C_nH_{(2n+2)} + nH_2O$ 4.1

Water gas shift reaction: $CO + H_2O \rightleftharpoons CO_2 + H_2$ 4.2

In case of 10Co_commercial ZSM-5 (porous) and 10Co_ZSM-5_Si/Al 20, They present similar methane selectivity which is 94.20 and 93.10 % that illustrated in table 4.9 resulting from the same Si/Al ratio but the 10Co_ZSM-5_Si/Al 20 is slightly lower due to large cobalt particle size and low surface area.

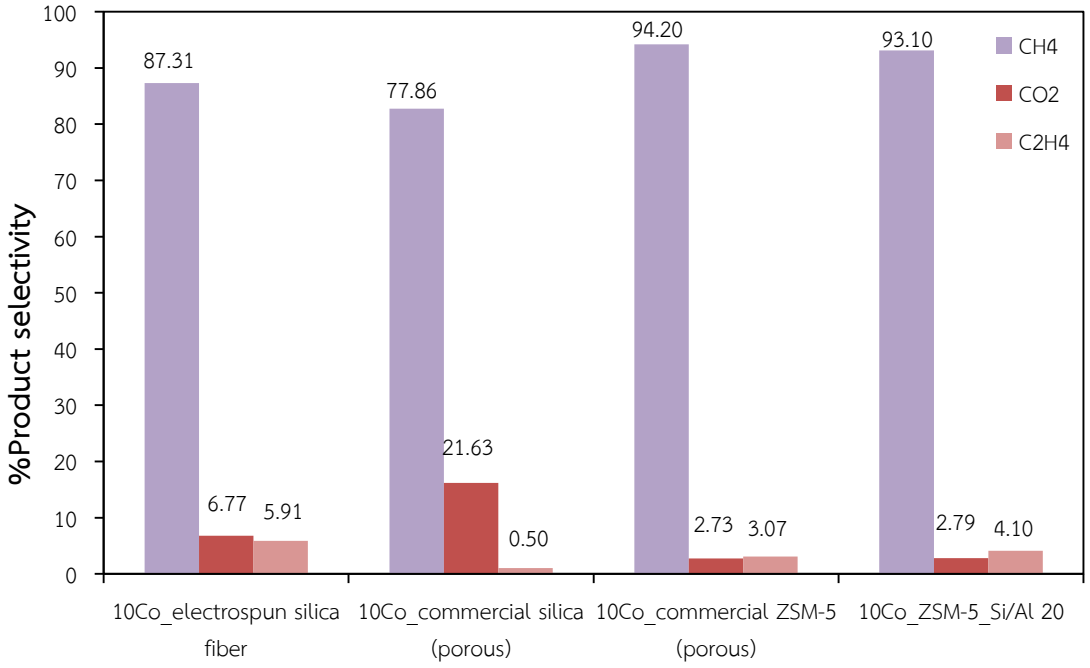

Fig. 4.24 %Product selectivity of 10Co_electrospun silica fiber, 10Co_commercial silica (porous), 10Co_commercial ZSM-5 (porous) and 10Co_ZSM-5_Si/Al 20 with reaction time 0 to 190 minutes.

Table 4.9 is the conclusion of %CO conversion, % products selectivity (CH_4, CO_2 and C_2H_4) with various Si/Al ratio and support types. 10Co_commercial silica porous exhibits highest CO conversion with 95.48%. The electrospun silica fiber has lower CO conversion comparing to commercial silica (porous) due to its small surface area. The CO conversion of fibrous form of ZSM-5 catalysts with Si/Al ratios 20 to 80 are ranging from 34.29 to 42.99% whereas commercial ZSM-5 catalyst is 36.71%. The CH_4 selectivity of fibrous form ZSM-5 catalysts with SI/Al ratios 20 to 80 is ranging from 88.33 to 93.10 % and tends to decrease at higher Si/Al ratios.

Table 4.9 %CO conversion and %products selectivity (CH_4, CO_2 and C_2H_4) with various Si/Al ratio and support types.

Catalyst	%CO conversion	% Product selectivity		
		CH_4	CO_2	C_2H_4
10Co_electrospun silica fiber	31.38	87.31	6.77	5.91
10Co_commercial silica (porous)	95.48	77.86	21.63	0.50
10Co_commercial ZSM-5 (porous)	36.71	94.20	2.73	3.07
10Co_ZSM-5_Si/Al 20 fiber	34.29	93.10	2.79	4.10
10Co_ZSM-5_Si/Al 40 fiber	36.08	92.79	2.90	4.31
10Co_ZSM-5_Si/Al 60 fiber	37.01	88.68	7.20	4.11
10Co_ZSM-5_Si/Al 80 fiber	42.99	88.33	7.27	4.40

CHAPTER V

CONCLUSION AND RECOMMENDATION

5.1 Conclusion

The ZSM-5 on electrospun silica fiber was successfully prepared by electrospinning and hydrothermal method. The prepared electrospun silica fiber with needle size 0.55 mm, TCD 10 cm, applied voltage 15 kV and spinning rate 10 ml/h has average diameter 0.68 μm and small surface area 3.7950 m^2/g. ZSM-5 deposition on electrospun silica fiber was performed at pH of solution equal to 9 with hydrothermal condition 180 °C for 24 hours and studied the effect of Si/Al ratio for zeolite coating. The increasing of Si/Al ratio from 20 to 80 yielded more zeolite coating resulting in the increasing of BET surface area from 70.74 - 277.80 m^2/g. All prepared samples were confirmed the ZSM-5 crystal structure by XRD technique, the XRD patterns showed two characteristic peaks at 2 theta between 7-10 and 22-25 corresponding to the MFI structure. The catalytic properties of ZSM-5 on electrospun silica fiber were investigated with CO hydrogenation reaction by loading 10% of Co and compared between different Si/Al ratios including different support types (SiO_2 porous, electrospun silica fiber and commercial ZSM-5 porous). These catalysts were characterized by SEM, EDX, XRD and TPR prior catalytic testing. The EDX can confirm that the catalyst contained Si, Al and Co element. The XRD results revealed that there is Co_3O_4 composing in the catalyst and the cobalt particle size was also measured. The TPR profiles at 300 – 500 °C indicated the reduction of $Co_3O_4 \rightarrow CoO \rightarrow Co^0$ and the higher region over 650 °C indicated the less reducibility of cobalt species like cobalt silicates phase or forming strong Co-O-Al bond. The reduction behavior of fibrous catalyst usually occurred at lower temperature and contained high degree of reduction comparing with SiO_2 porous and commercial ZSM-5 porous that means the fibrous catalyst more easily reduced. The decreasing of Si/Al ratio led to strong interaction between cobalt particle and the support yielding the smaller cobalt particle and decreasing of reducibility. The highest CO conversion was found in SiO_2 porous due to high surface area and large cobalt particle size whereas commercial ZSM-5 porous yielded lower due to the effect of aluminium content. The degree of CO conversion decreasing from 95.48 to 34.29% which can be ordered as follow: 10Co_commercial silica (porous) > 10Co_ZSM-5_Si/Al 80 > 10Co_ZSM-5_Si/Al 60 > 10Co_ZSM-5_Si/Al 40 > 10Co_ZSM-5_Si/Al 20 > 10Co_commercial ZSM-

5 (porous) >10Co_electrospun silica fiber. The methane selectivity correlated with acidity on the support and the particle size of the metal. The 10Co_ZSM-5_Si/Al 20 and 10Co_commercial ZSM-5 (porous) exhibit closely methane selectivity which are 93.10 and 94.20% that higher than others due to increasing acidity on the support and having small cobalt particle size.

5.2 Recommendation

Although ZSM-5 deposited on electrospun silica fiber is successfully prepared but this technique requires gel coating on the fiber that consumes large amount of organic template (TPAOH). Therefore preparation without organic template or without gel coating should be developed for cost reduction. The conditions for ZSM-5 preparation are still determined to control the level of crystal growth on fiber such as aging temperature, aging time and sequence of solution mixing. Furthermore, the deposition of other zeolite on electrospun silica fiber is also attractive choice for a wide range of applications.

REFERENCES

[1] Sang, S., Chang, F., Liu, Z., He, C., He, Y., and Xu, L. Difference of ZSM-5 zeolites synthesized with various templates. Catalysis Today 93–95(0) (2004): 729-734.

[2] Hagen, J. Industrial Catalysis: A Practical Approach. Wiley, 2006.

[3] Payra, P. and Dutta, P. Zeolites: A primer. in Handbook of Zeolite Science and Technology, pp. 1-19. U.S.A.: CRC Press, 2003.

[4] Afandizadeh, S. and Foumeny, E.A. Design of packed bed reactors: guides to catalyst shape, size, and loading selection. Applied Thermal Engineering 21(6) (2001): 669-682.

[5] Jansen, J.C., et al. Zeolitic coatings and their potential use in catalysis. Microporous and Mesoporous Materials 21(4–6) (1998): 213-226.

[6] Matatov-Meytal, Y. and Sheintuch, M. Catalytic fibers and cloths. Applied Catalysis A: General 231(1–2) (2002): 1-16.

[7] Newton Luiz Dias, F. and Devaney Ribeiro do, C. Adsorption at Silica, Alumina, and Related Surfaces. in Somasundaran, P. (ed.)Encyclopedia of Surface and Colloid Science, Second Edition, pp. 209-228. U.S.A.: CRC Press, 2007.

[8] Georgiev, D., Bogdanov, B., Angelova, K., Markovska, I., and Hristov, Y. Synthetic zeolites - structure, classification, current trend in zeolite synthesis review. in Economics and Society development on the Base of Knowledge, pp. 1-5. Bulgaria: Technical studies, 2009.

[9] Gaag, F.J.v.d. ZSM-5 type zeolites: synthesis and use in gasphase reactions with ammonia. dokter, scheikundig ingenieur Technische Universiteit Delft, 1987.

[10] Singh, R. and Dutta, P.K. MFI: A case study of zeolite synthesis. in Handbook of Zeolite Science and Technology, p. 1204. U.S.A.: CRC Press, 2003.

[11] Byrappa, K. and Yoshimura, M. 6 - Hydrothermal Synthesis and Growth of Zeolites. in Byrappa, K. and Yoshimura, M. (eds.),Handbook of Hydrothermal Technology (Second Edition), pp. 269-347. Oxford: William Andrew Publishing, 2013.

[12] Cundy, C.S. and Cox, P.A. The hydrothermal synthesis of zeolites: Precursors, intermediates and reaction mechanism. Microporous and Mesoporous Materials 82(1–2) (2005): 1-78.

[13] Cundy, C.S., Forrest, J.O., and Plaisted, R.J. Some observations on the preparation and properties of colloidal silicalites. Part I: synthesis of colloidal

silicalite-1 and titanosilicalite-1 (TS-1). Microporous and Mesoporous Materials 66(2–3) (2003): 143-156.

[14] Selvin, R., Hsu, H.-L., Roselin, L.S., and Bououdina, M. Effect of aging on the precursor sol for the synthesis of nanocrystalline ZSM-5. Synthesis and Reactivity in Inorganic, Metal-Organic, and Nano-Metal Chemistry 41(8) (2011): 1028-1032.

[15] Yu, J. Synthesis of zeoltes. in Introduction to Zeolite Molecular Sieves, pp. 39-103. UK: Elsevier Science, 2007.

[16] Deepesh, B., Radha, T., Purnima, K.S., Yogesh, G., and Pankaj, S. Hydrothermal synthesis and characterization of zeolite: effect of crystallization temperature. Research Journal of Chemical Sciences 3(9) (2013): 1-4.

[17] Karimi, R., Bayati, B., Aghdam, N.C., Ejtemaee, M., and Babaluo, A.A. Studies of the effect of synthesis parameters on ZSM-5 nanocrystalline material during template-hydrothermal synthesis in the presence of chelating agent. Powder Technology 229 (2012): 229-236.

[18] Houssin, C.J.Y. Nanoparticles in Zeolite Synthesis. Ph.D., Technische Universiteit Eindhoven, 2003.

[19] Taek Jung, K., Chu, Y.-H., Haam, S., and Gun Shul, Y. Synthesis of mesoporous silica fiber using spinning method. Journal of Non-Crystalline Solids 298(2–3) (2002): 193-201.

[20] Krissanasaeranee, M., Vongsetskul, T., Rangkupan, R., Supaphol, P., and Wongkasemjit, S. Preparation of ultra-fine silica fibers using electrospun poly(vinyl alcohol)/silatrane composite fibers as precursor. Journal of the American Ceramic Society 91(9) (2008): 2830-2835.

[21] S.M., A., WANG, J., WU, G., SHEN, J., and MA, J. Review on sol-gel derived coatings: process, techniques and optical applications Journal of Materials Processing Technology 18(3) (2002): 211-218.

[22] Miao, J., Miyauchi, M., Simmons, T.J., Dordick, J.S., and Linhardt, R.J. Electrospinning of nanomaterials and applications in electronic components and devices. Journal of Nanoscience and Nanotechnology 10(9) (2010): 5507–5519.

[23] Huang, Z.-M., Zhang, Y.Z., Kotaki, M., and Ramakrishna, S. A review on polymer nanofibers by electrospinning and their applications in nanocomposites. Composites Science and Technology 63(15) (2003): 2223-2253.

[24] Frenot, A. and Chronakis, I.S. Polymer nanofibers assembled by electrospinning. Current Opinion in Colloid & Interface Science 8(1) (2003): 64-75.

[25] Pham, Q., Sharma, U., and Mikos, A.G. Electrospinning of polymeric nanofibers for tissue engineering applications: a review. Tissue Engineering 12(5) (2006): 1197-1211.

[26] Fengyu, L., Yong, Z., and Yanlin, S. Core-shell nanofibers: nano channel and capsule by coaxial electrospinning. in, 2010.

[27] Sakai, S., Kawakami, K., and Taya, M. Controlling the diameters of silica nanofibers obtained by sol–gel/electrospinning methods. Journal of Chemical Engineering of Japan 45(6) (2012): 436-440.

[28] Pirzada, T., Arvidson, S.A., Saquing, C.D., Shah, S.S., and Khan, S.A. Hybrid silica-PVA nanofibers via sol-gel electrospinning. Langmuir 28(13) (2012): 5834-5844.

[29] Liu, F., Guo, R., Shen, M., Wang, S., and Shi, X. Effect of processing variables on the morphology of electrospun poly[(lactic acid)-co-(glycolic acid)] nanofibers. Macromolecular Materials and Engineering 294(10) (2009): 666-672.

[30] Van Der Laan, G.P. and Beenackers, A.A.C.M. Kinetics and selectivity of the fischer–tropsch synthesis: a literature review. Catalysis Reviews 41(3-4) (1999): 255-318.

[31] Choosri, N., Swadchaipong, N., Utistham, T., and Hartley, U.W. Gasoline and diesel production via fischer-tropsch synthesis over cobalt based catalyst. World Academy of Science, Engineering and Technology (72) (2012): 1812-1816.

[32] Sarkari, M., Fazlollahi, F., Razmjooie, A., and Mirzaeid, A.A. Fisher-tropsch synthesis on alumina supported iron-nickel catalysts: effect of preparation methods. Chemical and Biochemical Engineering Quarterly 25(3) (2011): 289–297.

[33] De la Osa, A.R., De Lucas, A., Romero, A., Valverde, J.L., and Sánchez, P. Fischer–Tropsch diesel production over calcium-promoted Co/alumina catalyst: Effect of reaction conditions. Fuel 90(5) (2011): 1935-1945.

[34] Tsakoumis, N.E., Rønning, M., Borg, Ø., Rytter, E., and Holmen, A. Deactivation of cobalt based fischer–tropsch catalysts: a review. Catalysis Today 154(3–4) (2010): 162-182.

[35] Karre, A.V., Kababji, A., Kugler, E.L., and Dadyburjor, D.B. Effect of time on stream and temperature on upgraded products from Fischer–Tropsch

synthesis when zeolite is added to iron-based activated-carbon-supported catalyst. Catalysis Today 214(0) (2013): 82-89.

[36] Bukur, D.B., Lang, X., and Ding, Y. Pretreatment effect studies with a precipitated iron Fischer–Tropsch catalyst in a slurry reactor. Applied Catalysis A: General 186(1–2) (1999): 255-275.

[37] Dai, X. and Yu, C. Effects of pretreatment and reduction on the Co/Al_2O_3 catalyst for CO hydrogenation. Journal of Natural Gas Chemistry 17(3) (2008): 288-292.

[38] Liu, Y., Hanaoka, T., Miyazawa, T., Murata, K., Okabe, K., and Sakanishi, K. Fischer–Tropsch synthesis in slurry-phase reactors over Mn- and Zr-modified Co/SiO_2 catalysts. Fuel Processing Technology 90(7–8) (2009): 901-908.

[39] Steen, E.v., et al. TPR Study on the Preparation of Impregnated Co/SiO_2 Catalysts. Journal of Catalysis 162(2) (1996): 220-229.

[40] Sartipi, S., et al. Hierarchical H-ZSM-5-supported cobalt for the direct synthesis of gasoline-range hydrocarbons from syngas: Advantages, limitations, and mechanistic insight. Journal of Catalysis 305(0) (2013): 179-190.

[41] Dalil, M., Sohrabi, M., and Royaee, S.J. Application of nano-sized cobalt on ZSM-5 zeolite as an active catalyst in Fischer–Tropsch synthesis. Journal of Industrial and Engineering Chemistry 18(2) (2012): 690-696.

[42] Kang, S.-H., et al. ZSM-5 supported cobalt catalyst for the direct production of gasoline range hydrocarbons by fischer–tropsch synthesis. Catalysis Letters 141(10) (2011): 1464-1471.

[43] Kang, J.S., et al. Nano-sized cobalt based fischer-tropsch catalysts for gas-to-liquid process applications. Journal of Nanoscience and Nanotechnology 10(5) (2010): 3700-4.

[44] Yang, G., He, J., Yoneyama, Y., and Tsubaki, N. H-ZSM-5/cobalt/silica capsule catalysts with different crystallization time for direct synthesis of isoparaffins: simultaneous realization of space confinement effect and shape selectivity effect. in Fábio Bellot Noronha, M.S. and Eduardo Falabella, S.-A. (eds.),Studies in Surface Science and Catalysis, pp. 73-78: Elsevier, 2007.

[45] Yang, G., He, J., Yoneyama, Y., Tan, Y., Han, Y., and Tsubaki, N. Preparation, characterization and reaction performance of H-ZSM-5/cobalt/silica capsule catalysts with different sizes for direct synthesis of isoparaffins. Applied Catalysis A: General 329(0) (2007): 99-105.

[46] Yodwanlop, P. Preparation of Co/SiO_2 fiber by electrospinning technique for fischer-tropsch synthesis. M.Sc., Department of Chemical Technology, Faculty of Science Chulalongkorn, 2010.

[47] Louis, B., Tezel, C., Kiwi-Minsker, L., and Renken, A. Synthesis of structured filamentous zeolite materials via ZSM-5 coatings of glass fibrous supports. Catalysis Today 69(1–4) (2001): 365-370.

[48] Choi, S.-S., Lee, S., Im, S., Kim, S., and Joo, Y. Silica nanofibers from electrospinning/sol-gel process. Journal of Materials Science Letters 22(12) (2003): 891-893.

[49] Promduang, S. Preparation of Co/SiO_2 fiber catalysts by electrospinning for CO Hydrogenation. M.Sc., Department of Petrochemistry and Polymer Science, Faculty of Science Chulalongkorn University, 2010.

[50] Paik, U., Kim, J.P., and Jung, Y.S. The effect of Si dissolution on the stability of silica particles and its influence on chemical mechanical polishing for interlayer dielectrics. J. Korean Phys. Soc. 39(Suppl. S) (2001): S201-S204.

[51] Li, Y., Zhang, X., and Wang, J. Preparation for ZSM-5 membranes by a two-stage varying-temperature synthesis. Separation and Purification Technology 25(1–3) (2001): 459-466.

[52] Petushkov, A., Yoon, S., and Larsen, S.C. Synthesis of hierarchical nanocrystalline ZSM-5 with controlled particle size and mesoporosity. Microporous and Mesoporous Materials 137(1–3) (2011): 92-100.

[53] Majano, G., Darwiche, A., Mintova, S., and Valtchev, V. Seed-induced crystallization of nanosized Na-ZSM-5 crystals. Industrial & Engineering Chemistry Research 48(15) (2009): 7084-7091.

[54] Xu, F., et al. Rapid tuning of ZSM-5 crystal size by using polyethylene glycol or colloidal silicalite-1 seed. Microporous and Mesoporous Materials 163(0) (2012): 192-200.

[55] Rebrov, E.V., Mies, M.J.M., de Croon, M.H.J.M., and Schouten, J.C. chapter 12 - hydrothermal synthesis of zeolitic coatings for applications in micro-structured reactors. in Valtchev, V., Mintova, S., and Tsapatsis, M. (eds.),Ordered Porous Solids, pp. 311-334. Amsterdam: Elsevier, 2009.

[56] Shirazi, L., Jamshidi, E., and Ghasemi, M.R. The effect of Si/Al ratio of ZSM-5 zeolite on its morphology, acidity and crystal size. Crystal Research and Technology 43(12) (2008): 1300-1306.

[57] Lin, J.-C. and Chao, K.-J. Distribution of silicon-to-aluminium ratios in zeolite ZSM-5. Journal of the Chemical Society, Faraday Transactions 1: Physical Chemistry in Condensed Phases 82(9) (1986): 2645-2649.

[58] Ali, M.A., Brisdon, B., and Thomas, W.J. Synthesis, characterization and catalytic activity of ZSM-5 zeolites having variable silicon-to-aluminum ratios. Applied Catalysis A: General 252(1) (2003): 149-162.

[59] Yang, G., et al. Tandem catalytic synthesis of light isoparaffin from syngas via Fischer–Tropsch synthesis by newly developed core–shell-like zeolite capsule catalysts. Catalysis Today 215(0) (2013): 29-35.

[60] Silva, V.J., Rodrigues, J.J., Soares, R.R., Napolitano, M.N., and Rodrigues, M.G.F. Cobalt supported on ZSM-5 zeolite using kaolin as silicon and aluminum sources for Fischer-tropsch synthesis. Brazilian Journal of Petroleum and Gas 7(2) (2013): 87.

[61] Vishwanathan, V. and Narayanan, S. Role of zeolite supported metal systems in the conversion of CO (Hydrogenation) to hydrocarbons. Journal of Scientific and Industrial Research 46 (1987): 433-437.

[62] Fischer, N., van Steen, E., and Claeys, M. Structure sensitivity of the Fischer–Tropsch activity and selectivity on alumina supported cobalt catalysts. Journal of Catalysis 299(0) (2013): 67-80.

[63] Ngamcharussrivichai, C., Liu, X., Li, X., Vitidsant, T., and Fujimoto, K. An active and selective production of gasoline-range hydrocarbons over bifunctional Co-based catalysts. Fuel 86(1–2) (2007): 50-59.

APPENDIX

Appendix A

Calculation for preparation of electrospun silica fiber

Mol ratio 1 TEOS: 2 EtOH: $2H_2O$: 0.0144 HCl

Starting from H_2O 3 ml

∴ mol H_2O

$$= 3 \text{ ml} \times \frac{1 \text{ g}}{1 \text{ ml}} \times \frac{1 \text{ mol}}{18 \text{ g}}$$

$$= 0.1667 \text{ mol}$$

ml of TEOS (calculate from concentration 100%)

$$= \frac{3 \text{ ml } H_2O}{18 \text{ g/mol } H_2O} \times \frac{1 \text{ g } H_2O}{1 \text{ ml } H_2O} \times \frac{1 \text{ mol TEOS}}{2 \text{ mol } H_2O} \times \frac{208.33 \text{ g TEOS}}{1 \text{ mol TEOS}} \times \frac{1 \text{ ml TEOS}}{0.94 \text{ g TEOS}}$$

$$= 18.02 \text{ ml}$$

ml of EtOH (calculate from concentration 100%)

$$= \frac{3 \text{ ml } H_2O}{18 \text{ g/mol } H_2O} \times \frac{1 \text{ g } H_2O}{1 \text{ ml } H_2O} \times \frac{2 \text{ mol EtOH}}{2 \text{ mol } H_2O} \times \frac{46.07 \text{ g EtOH}}{1 \text{ mol EtOH}} \times \frac{1 \text{ ml TEOS}}{0.79 \text{ g TEOS}}$$

$$= 9.72 \text{ ml}$$

ml of HCl (calculate from concentration 37 %)

$$= \frac{3 \text{ ml } H_2O}{18 \text{ g/mol } H_2O} \times \frac{1 \text{ g } H_2O}{1 \text{ ml } H_2O} \times \frac{0.0144 \text{ mol HCl}}{2 \text{ mol } H_2O} \times \frac{36.46 \text{ g HCl}}{1 \text{ mol HCl}} \times \frac{1 \text{ ml HCl}}{1.18 \text{ g HCl}} \times \frac{1}{0.37}$$

$$= 0.10 \text{ ml}$$

Calculation for ZSM-5 preparation

Mol ratio 1 TEOS: 0.25 TPAOH: 0.0250 $Al(NO_3)_3.9H_2O$: 80 H_2O. (Si/Al 40)

Starting from H_2O 30 ml

∴ mol H_2O

$$= 30 \text{ ml} \times \frac{1 \text{ g}}{1 \text{ ml}} \times \frac{1 \text{ mol}}{18 \text{ g}}$$

$$= 1.67 \text{ mol}$$

g of $Al(NO_3)_3.9H_2O$

$$= 0.0250 \text{ mol } Al(NO_3)_3.9H_2O \times \frac{375.134 \text{ g}}{1 \text{ mol}} \times \frac{30 \text{ ml } H_2O}{18 \text{ g/mol } H_2O} \times \frac{1 \text{ g } H_2O}{1 \text{ ml } H_2O} \times \frac{1}{80 \text{ mol } H_2O}$$

= 0.1953 g

ml of TEOS (calculate from concentration 100%)

$$= \frac{30 \text{ ml } H_2O}{18 \text{ g/mol } H_2O} \times \frac{1 \text{ g } H_2O}{1 \text{ ml } H_2O} \times \frac{1 \text{ mol TEOS}}{80 \text{ mol } H_2O} \times \frac{208.33 \text{ g TEOS}}{1 \text{ mol TEOS}} \times \frac{1 \text{ ml TEOS}}{0.94 \text{ g TEOS}}$$

= 4.63 ml

ml of TPAOH (calculate from concentration 20.34 %)

$$= \frac{30 \text{ ml } H_2O}{18 \text{ g/mol } H_2O} \times \frac{1 \text{ g } H_2O}{1 \text{ ml } H_2O} \times \frac{0.25 \text{ mol TPAOH}}{80 \text{ mol } H_2O} \times \frac{203.37 \text{ g TPAOH}}{1 \text{ mol TPAOH}} \times \frac{1}{0.2034}$$

= 5.22 ml

Calculation of Co loading

Deposition of 10%wt Co on 0.1 g electrospun silica

Electrospun silica 90 g compose of Co 10 g

Electrospun silica 0.1 g compose of Co (10×0.1) ÷ 90 = 0.01 g

Molecular weight of Co = 58.93 g/mol

Molecular weight of $Co(NO_3)_2.6H_2O$ = 291.03 g/mol

If Co 58.93 g, weight $Co(NO_3)_2.6H_2O$ = 291.03 g

Thus Co 0.01 g, weight $Co(NO_3)_2.6H_2O$ = (291.03 × 0.01) ÷58.93 = 0.0494 g

Deposition of 10%wt Co on SiO_2 porous by wet impregnation

Loading 10%wt of Co into 5 g of SiO_2 porous

SiO_2 porous 90 g compose of Co 10 g

SiO_2 porous 5 g compose of Co (10×5) ÷ 90 g = 0.5560 g

If require Co 58.93 g, weight $Co(NO_3)_2.6H_2O$ 291.03 g

If require Co 0.5560 g, weight $Co(NO_3)_2.6H_2O$ = (291.03×0.556) ÷58.93 = 2.7458 g

Pore volume of SiO_2 porous = 1.12 ml/g

∴ If prepare 5 g of catalyst, the solution should be 1.12 × 5 = 5.6 ml

Deposition of 10%wt Co on ZSM-5 porous by wet impregnation

Loading 10%wt of Co into 5 g of ZSM-5 porous

ZSM-5 porous 90 g compose of Co 10 g

ZSM-5 porous 5 g compose of Co (10×5) ÷ 90 g = 0.5560 g

If require Co 58.93 g, weight $Co(NO_3)_2.6H_2O$ 291.03 g

If require Co 0.5560 g, weight $Co(NO_3)_2.6H_2O$ = (291.03 ×0.556) ÷58.93 = 2.7458 g

Pore volume of SiO_2 porous = 0.2248 ml/g

∴ If prepare 5 g of catalyst, the solution should be 0.2248 × 5 = 1.1240 ml

Calculation of % reduction

Catalyst: 10wt% Co/SiO_2 fiber catalyst

Flow rate of H_2 = 30.00 ml/min from 5% H_2 balanced in in N_2

∴ Flow rate of H_2 = 0.05 x 30.00 ml/min

= 1.50 ml H_2 /min

Calculated mol of H_2 (real)

$$n = \frac{Pv}{RT}$$

Where P = pressure (atm)

v = volume (ml/min)

R = 82.057 atm·ml/mol·K

T = temperature (K)

Thus mol H_2 /min = $\dfrac{1 \text{ atm} \times 1.50 \text{ ml/min}}{82.057 \text{ atm} \cdot \frac{\text{ml}}{\text{mol} \cdot \text{K}} \times 298 \text{ K}}$

= 6.1342×10^{-5} mol H_2 /min

Area of H_2 before reduced = 90442.1 area/min

= 6.3142×10^{-5} mol H_2 /min

Area of H_2 after reduced = 243846.70 area/min

mol H_2 /min = $\dfrac{243846.70 \text{ area /min} \times (6.3142 \times 10^{-5}) \text{ mol } H_2/\text{min}}{90442.1 \text{ area/min}}$

= 1.6538×10^{-4} mol H_2 /min (real)

Weight 10% of cobalt on 0.1 g electrospun silica fiber

Molecular weight of Co = 58.93 g/mol

10 % by weight of cobalt in the 0.1 g of electrospun silica fiber

= (0.1 × 10) ÷100 = 0.01 g

= 0.01÷58.93 = 0.00017 mol

From equation $Co_3O_4 + 4H_2 \rightarrow 3Co + 4H_2O$

Ratio 1 : 4 : 3 : 4

$$\frac{0.00017}{3} : \frac{0.00017}{4} : \frac{0.00017}{0.00017} : \frac{0.00017}{4}$$

0.0000566 : 0.000226 : 0.00017 : 0.0002266

mol H_2 (Theory) = 0.000226 mol

% reduction = [mol H_2 (real)/ mol H_2 (theory)] ×100

= $[(1.6538 \times 10^{-4}) \div (2.26 \times 10^{-4})] \times 100$ = 73.18 %

Calculation of CO conversion, CH_4 selectivity and CO_2 selectivity for CO hydrogenation

$$n = \frac{Pv}{RT}$$

Where P = pressure (atm)

v = volume (L)

n = mole (mol)

R = constant

T = temperature (K)

Catalyst 10% Co on electrospun silica fiber

Weight of catalyst 0.2 g

Temperature 298 K

Pressure 1 atm

R constant 0.0820513 atm ▪ L/mol ▪ K

Volume input (V_{in}) 0.015 L/min

mol input synthesis gas ($n_{in,syn\ gas}$)

$$= \frac{1\ atm \times 0.010\ L/min}{0.0820513\ atm \cdot \frac{ml}{mol \cdot K} \times 298\ K}$$

= 0.000409 mol/min = 0.024538 mol/ h

mol input H_2 ($n_{in,Hydrogen}$)

$$= \frac{1\ atm \times 0.005\ L/min}{0.0820513\ atm \cdot \frac{ml}{mol \cdot K} \times 298\ K}$$

= 0.000204 mol/min = 0.012269 mol/ h

mol input (n_{in})

$$= \frac{1 \text{ atm} \times 0.015 \text{ L/min}}{0.0820513 \text{ atm} \cdot \frac{\text{ml}}{\text{mol} \cdot \text{K}} \times 298 \text{ K}}$$

= 0.000613 mol/min = 0.036808 mol/ h

W/F (g•h/mol) = (0.2÷0.036808) = 5.433618

Reactant component	percent	mol
H_2	65	= (65 × 0.000613)÷100 = 0.000196
CO	32	= (32 × 0.000613) ÷100 = 0.0003990
Ar	3	= (3 × 0.000613) ÷100 = 1.84×10^{-5}
Volume output (V_{out})	0.015 L/min	

mol output (n_{out})

$$= \frac{1 \text{ atm} \times 0.015 \text{ L/min}}{0.0820513 \text{ atm} \cdot \frac{\text{ml}}{\text{mol} \cdot \text{K}} \times 298 \text{ K}}$$

= 0.000613 mol/min = 0.036808 mol/ h

Area of synthesis gas before reaction

No.	Area			
	H_2	Ar	CO	CO/Ar
1	23860.2	133883	642077	4.7958
2	23936.3	124112	644817	5.1954
3	23577.3	141158	638531	4.5235
AVG	23756.8	132635	641674	4.8383

Area of synthesis gas after 20 minute of reaction

Area						
H_2	Ar	CO	CH_4	CO_2	C_2H_4	CO/Ar
22106.7	194250	618800	25888.9	2463.2	2349.9	3.1856

%CO conversion = [(4.8383 - 3.1856) ÷ 4.8383] x 100

= 34.15 %

Area of standard gas

STD	CH_4	CO	CO_2	C_2H_4
%	1.04	1.02	1.01	1
area1	17050.2	2207038	24417.1	23393.1
area2	17613.5	2237111	23644.5	21555
average	17331.9	2222075	24030.8	22474.1

$$n = \frac{Pv}{RT}$$

Where P = pressure (atm)

v = volume (L)

n = mole (mol)

T = temperature (K)

R = constant

mol CO_{out} = [(3.1856 x 132635) x 1.02] ÷ 2222075 = 0.1940%

= [(0.1940 ÷ 100)] x 0.015] ÷ [298 x 0.0820513]

= 1.1901×10^{-6} mol/min

mol CH_4 = (25888.9 x 1.04) ÷17331.9 = 1.5535%

= (1.5535 ÷ 100) x 0.015] ÷ [298 x 0.0820513]

= 9.5299×10^{-6} mol/min

mol CO_2 = (2463.2 x 1.01) ÷ 24030.8 = 0.1035%

= (0.1035 ÷ 100) x 0.015] ÷ [298 x 0.0820513]

= 6.3510×10^{-7} mol/min

mol C_2H_4 = (2349.9 x 1.00) ÷ 22474.1 = 0.1046%

= (0.1046 ÷ 100) x 0.015] ÷ [298 x 0.0820513]

= 6.4140×10^{-7} mol/min

mol total product = mol CO+ mol CH_4 +mol CO_2+ mol C_2H_4

= 1.081×10^{-5}

∴ CH_4 Selectivity = $[(9.5299 \times 10^{-6}) \div (1.081 \times 10^{-5})] \times 100$

= 88.16 %

∴ CO_2 Selectivity = $[(6.3510 \times 10^{-7}) \div (1.081 \times 10^{-5})] \times 100$ = 5.88 %

Appendix B

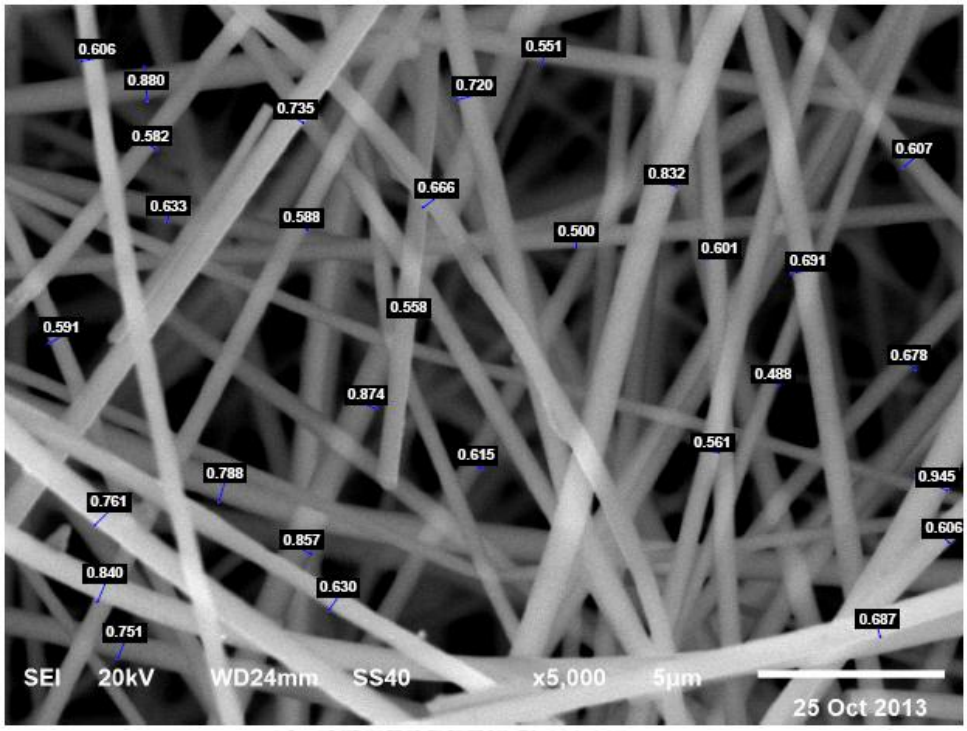

Fig. B-1 The measurement of electrospun silica fiber diameter by SemAfore.

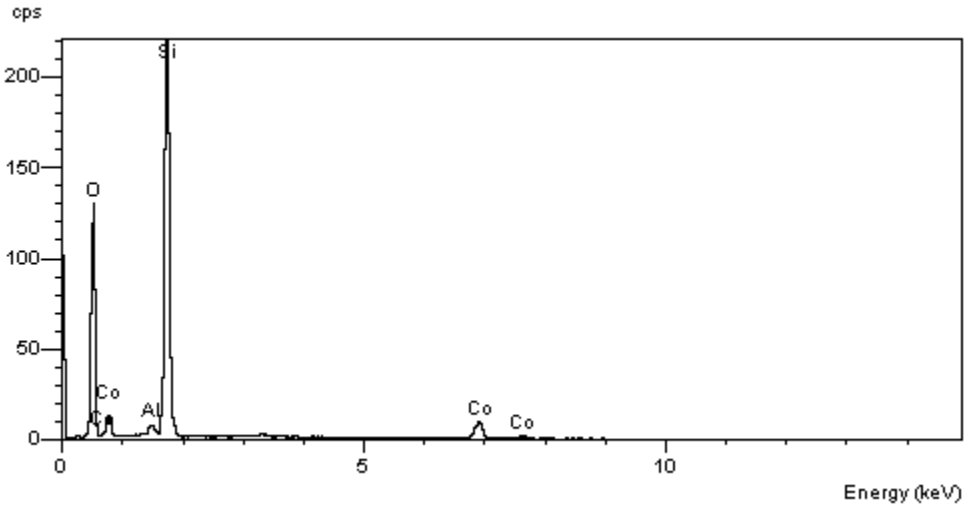

Fig. B-2 The component of 10Co_ZSM-5_Si/Al 20 measured by EDX.

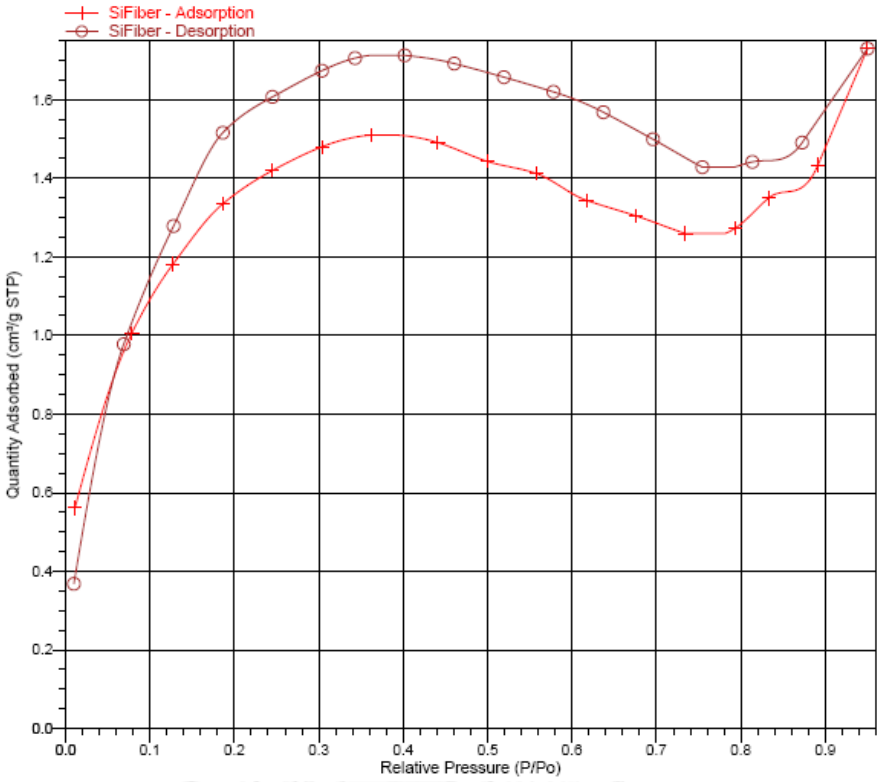

Fig. B-3 N_2 physisorption of electrospun silica fiber.

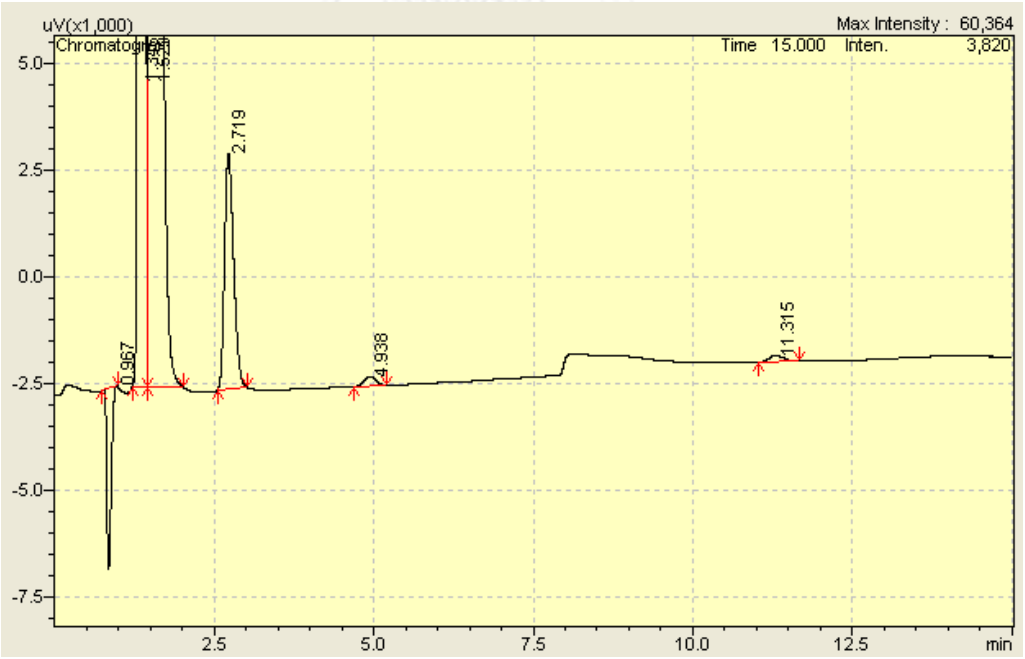

Fig. B-4 The signal of products analyzed by Gas chromatograph (GC).

Table B-1 Measurement of %CO conversion and product selectivity of 10Co_electrospun silica fiber performed with reaction temperature 280 C, H_2/CO 2:1 and space velocity = 75 ml/min/g catalyst.

Area	STD	10	30	50	70	90	110	130	150	170	190
H_2		22106.7	21650.3	21566	21478.9	21523	21599.3	21584.1	21068.3	21145.3	21591.7
Ar		194250	187985.3	187064.6	186031	185309.7	184627.1	183877.4	196010.4	183882	185530.7
CO	2222074.55	618799.5	624074.9	623962.3	622037.1	621818.5	622126.1	621700.5	625068	621602.3	619717.4
CH_4	17331.85	25888.9	25178.6	24741.8	24481.3	24077.4	23561.9	23078.6	25346.2	22643.3	22232.7
CO_2	24030.8	2463.2	2541.2	2568	2602.5	2756.2	2695.5	2762.7	2688.3	2890.2	2909.4

Minutes		10	30	50	70	90	110	130	150	170	190
mol	CO	0.0000012	0.0000012	0.0000012	0.0000012	0.0000013	0.0000013	0.0000013	0.0000012	0.0000013	0.0000012
	CH_4	9.5293E-06	9.2679E-06	9.1071E-06	9.0112E-06	8.8625E-06	8.6728E-06	8.4949E-06	9.3295E-06	8.3347E-06	8.1835E-06
	CO_2	6.3506E-07	6.5517E-07	6.6208E-07	6.7097E-07	7.1060E-07	6.9495E-07	7.1227E-07	6.9309E-07	7.4514E-07	7.5009E-07
% CO conversion		34.16	31.38	31.06	30.89	30.65	30.35	30.12	34.09	30.13	30.96
% Selectivity	CH_4	88.19	87.59	87.67	87.45	87.16	87.09	86.92	87.81	86.31	86.34
	CO_2	5.88	6.19	6.37	6.51	6.99	6.98	7.29	6.52	7.72	7.91

Table B-2 Measurement of % CO conversion and product selectivity of 10Co_commercial silica (porous) performed with reaction temperature 280 °C, H_2/CO 2:1 and space velocity = 75 ml/min/g catalyst.

Area	STD	10	30	50	70	90	110	130	150	170	190
H_2		5029.1	5868.9	6290.1	6847.5	7149.3	8185	8788.9	9718.9	10206.5	15879.6
Ar		445626.9	425234.7	417280.7	402666.9	397029.8	387174.8	378767.5	367612.1	352796.8	297128.3
CO	2159042.1	17810.1	18751.6	16848	18559.5	21682.8	24984.7	29538.8	39021.9	68898.2	284085.7
CH_4	17236.5	677979.6	656728.4	634403.9	614809.4	594352.9	566085.8	548590.1	527536.4	496162.6	357780.1
CO_2	20443.5	173957	181419.5	186945.3	192500.5	196322	209807.4	203193.5	205872.6	203461.4	156074.1

Minutes		10	30	50	70	90	110	130	150	170	190
mol	CO	0.0000000	0.0000000	0.0000000	0.0000000	0.0000000	0.0000000	0.0000000	0.0000001	0.0000001	0.0000005
	CH_4	2.5093E-04	2.4307E-04	2.3481E-04	2.2755E-04	2.1998E-04	2.0952E-04	2.0304E-04	1.9525E-04	1.8364E-04	1.3242E-04
	CO_2	5.2197E-05	5.4436E-05	5.6094E-05	5.7761E-05	5.8908E-05	6.2954E-05	6.0970E-05	6.1774E-05	6.1050E-05	4.6831E-05
%CO conversion		98.89	98.77	98.88	98.72	98.48	98.20	97.83	97.05	94.57	73.40
% Selectivity	CH_4	82.65	81.46	80.45	79.46	78.56	76.52	76.48	75.51	74.48	73.09
	CO_2	17.19	18.24	19.22	20.17	21.04	22.99	22.96	23.89	24.76	25.85

Table B-3 Measurement of %CO conversion and product selectivity of 10Co_commercial ZSM-5 (porous) performed with reaction temperature 280 C, H_2/CO 2:1 and space velocity = 75 ml/min/g catalyst.

Area	STD	10	30	50	70	90	110	130	150	170	190
H_2		19984.9	19491	19588.2	19324	19246	18855	18912.2	19025.3	19590.2	19099.2
Ar		200909.9	195778.5	195615.3	194655.6	193876	191793.5	192252.3	192090.2	192073.7	191931.8
CO	2157869.9	593516.4	594976.4	595578.3	594520.4	595106.8	596302.7	597345.1	600295.6	602201.6	603210.9
CH_4	16879	60743.4	63243.3	64180.4	63196.2	62684.8	61580.2	60876	59738.6	58784.9	57659.3
CO_2	23353.95	2146.4	2453.4	2580.2	2710.6	2547.3	2916.5	2514.3	2586.2	2641.4	2402.2

Minutes		10	30	50	70	90	110	130	150	170	190
mol	CO	0.0000011	0.0000011	0.0000011	0.0000011	0.0000011	0.0000012	0.0000012	0.0000012	0.0000012	0.0000012
	CH_4	2.2959E-05	2.3903E-05	2.4258E-05	2.3886E-05	2.3692E-05	2.3275E-05	2.3009E-05	2.2579E-05	2.2218E-05	2.1793E-05
	CO_2	5.6378E-07	6.4442E-07	6.7772E-07	7.1197E-07	6.6908E-07	7.6606E-07	6.6041E-07	6.7930E-07	6.9380E-07	6.3097E-07
%CO conversion		39.26	37.51	37.40	37.20	36.89	36.07	36.11	35.74	35.53	35.38
% selectivity	CH_4	94.10	94.18	94.70	93.97	94.48	94.09	94.17	94.04	93.90	94.40
	CO_2	2.31	2.54	2.65	2.80	2.67	3.10	2.70	2.83	2.93	2.73

Table B-4 Measurement of %CO conversion and product selectivity of 10Co_ZSM-5_Si/Al 20 fiber performed with reaction temperature 280 C, H_2/CO 2:1 and space velocity = 75 ml/min/g catalyst.

Area	STD	10	30	50	70	90	110	130	150	170	190
H_2		19403.3	19431.2	19413.5	19170.1	19324.6	19440.3	19515.8	19505.9	19499.3	19568.9
Ar		201340	194949.4	193998	193881.9	192774.2	192561.6	191673.5	192001.3	192476	190815.3
CO	2158573.3	591033.2	594305.9	594914.2	596742.3	594894.5	590413.2	588351.9	587087.9	583514.3	583871.7
CH_4	17346.15	61154.6	57139.4	56591.6	54658.8	54471.6	53789.8	54586.2	54104.4	54192.4	54120.9
CO_2	23749.15	2683.2	2577	2076.2	3155	2142.2	1286	2590	2408	2307.6	2526.2

Minutes		10	30	50	70	90	110	130	150	170	190
mol	CO	0.0000011	0.0000012	0.0000012	0.0000012	0.0000012	0.0000012	0.0000012	0.0000012	0.0000012	0.0000012
	CH_4	2.2492E-05	2.1015E-05	2.0813E-05	2.0102E-05	2.0034E-05	1.9783E-05	2.0076E-05	1.9899E-05	1.9931E-05	1.9905E-05
	CO_2	6.9305E-07	6.6562E-07	5.3627E-07	8.1491E-07	5.5331E-07	3.3216E-07	6.6898E-07	6.2197E-07	5.9604E-07	6.5250E-07
% CO conversion		36.76	34.32	33.93	33.69	33.52	33.94	33.87	34.12	34.69	34.08
%Selectivity	CH_4	93.10	92.81	93.33	91.73	93.22	94.26	92.76	93.16	93.48	93.19
	CO_2	2.87	2.94	2.40	3.72	2.57	1.58	3.09	2.91	2.80	3.05

Table B-5 Measurement of %CO conversion and product selectivity of 10Co_ZSM-5_Si/Al 40 fiber performed with reaction temperature 280 C, H_2/CO 2:1 and space velocity = 75 ml/min/g catalyst.

Area	STD	10	30	50	70	90	110	130	150	170	190
H_2		19255.2	18956.4	18901.3	18993.9	19054	18914.4	19040.3	19070.4	19051.6	19007.1
Ar		207710	200648.3	198369.5	197028.3	194708.6	195631.2	194135	194500.4	193496	193422.9
CO	2160384.35	586986.7	590662.1	593598.1	594351.7	596992.3	596624.1	599455.1	599713	600516.5	600579
CH_4	17103.65	69940.6	66572.3	64199	62810.6	61895.8	60696.6	60142.4	60278.1	59034.5	58419.2
CO_2	23542.7	3078.4	3015.5	3007	2511	2828.9	2780.2	2677.5	2877.9	2768.2	2414.2

Minutes		10	30	50	70	90	110	130	150	170	190
mol	CO	0.0000011	0.0000011	0.0000011	0.0000011	0.0000012	0.0000011	0.0000012	0.0000012	0.0000012	0.0000012
	CH_4	2.6088E-05	2.4831E-05	2.3946E-05	2.3428E-05	2.3087E-05	2.2640E-05	2.2433E-05	2.2483E-05	2.2020E-05	2.1790E-05
	CO_2	8.0210E-07	7.8571E-07	7.8350E-07	6.5426E-07	7.3709E-07	7.2440E-07	6.9764E-07	7.4986E-07	7.2127E-07	6.2904E-07
% CO conversion		40.33	37.84	36.82	36.30	35.26	35.60	34.80	34.90	34.47	34.44
% Selectivity	CH_4	92.93	92.91	92.50	93.18	92.60	92.51	92.98	92.30	92.81	93.14
	CO_2	2.86	2.94	3.03	2.60	2.96	2.96	2.89	3.08	3.04	2.69

Table B-6 Measurement of %CO conversion and product selectivity of 10Co_ZSM-5_Si/Al 60 fiber performed with reaction temperature 280 C, H_2/CO 2:1 and space velocity = 75 ml/min/g catalyst.

Area	STD	10	30	50	70	90	110	130	150	170	190
H_2		20616	20355.3	20489.7	20513.8	20536.4	20726.4	20608.2	20748.8	20541.2	20677.9
Ar		191504.3	186976	184824.8	184348	183615.7	174423	182500.1	181643	180932.8	181146.9
CO	2174688.6	602208.2	604884.5	608941.7	608187.1	609719.1	600130.3	610180.5	611151.3	605887.2	610202.8
CH_4	17238.55	26158.2	23407.2	22647.8	21255.9	20198.6	19475.8	18818.8	17984.3	14358.2	16966.2
CO_2	20538.65	2550.8	1805.4	2214.1	1926.9	1896.3	2013.3	2060.3	1882.3	1680.4	1958.4

Minutes		10	30	50	70	90	110	130	150	170	190
mol	CO	0.0000011	0.0000011	0.0000011	0.0000011	0.0000011	0.0000012	0.0000011	0.0000012	0.0000011	0.0000012
	CH_4	9.6805E-06	8.6625E-06	8.3814E-06	7.8663E-06	7.4750E-06	7.2075E-06	6.9644E-06	6.6556E-06	5.3136E-06	6.2788E-06
	CO_2	7.6184E-07	5.3921E-07	6.6128E-07	5.7550E-07	5.6636E-07	6.0131E-07	6.1534E-07	5.6218E-07	5.0188E-07	5.8491E-07
% CO conversion		40.26	38.55	37.41	37.33	36.92	34.64	36.49	36.09	36.39	36.01
% Selectivity	CH_4	89.05	89.09	88.49	89.07	88.88	88.67	88.98	89.04	86.81	88.74
	CO_2	7.01	5.55	6.98	6.52	6.73	7.40	7.86	7.52	8.20	8.27

Table B-7 Measurement of %CO conversion and product selectivity of 10Co_ZSM-5_Si/Al 80 fiber performed with reaction temperature 280 C, H_2/CO 2:1 and space velocity = 75 ml/min/g catalyst.

Area	STD	10		30	50	70	90	110	130	150	170	190
H_2		18849.3	18702.3	19519.2	19667	19351.4	19768.5	19879.2	19879.2	20121.9	20202.7	
Ar		210905.2	198729.3	193954.2	191334.3	190925.7	190110	190413.2	190413.2	190832.6	190128	
CO	2161858.2	570729.8	580387	585141.6	593185.4	593251	596449	596421.9	596421.9	597593.6	597811.9	
CH_4	17409.3	79968.9	69265.1	57610.3	52969.9	50688.8	49160.9	47671.4	47671.4	45162.6	44006.5	
CO_2	21076.1	9317.5	5420.2	5381.3	5851.9	5326.8	5346.1	5127.7	5127.7	4742.6	4534.2	

Minute		10	30	50	70	90	110	130	150	170	190
mol	CO	0.0000009	0.0000010	0.0000010	0.0000010	0.0000010	0.0000010	0.0000010	0.0000010	0.0000010	0.0000010
	CH_4	2.9304E-05	2.5382E-05	2.1111E-05	1.9411E-05	1.8575E-05	1.8015E-05	1.7469E-05	1.7469E-05	1.6550E-05	1.6126E-05
	CO_2	2.7119E-06	1.5776E-06	1.5662E-06	1.7032E-06	1.5504E-06	1.5560E-06	1.4924E-06	1.4924E-06	1.3803E-06	1.3197E-06
% CO conversion		49.47	45.46	43.66	42.11	41.98	41.41	41.51	41.51	41.52	41.28
% Selectivity	CH_4	87.99	86.11	88.85	88.57	88.76	88.15	88.57	88.57	88.54	89.18
	CO_2	8.14	5.35	6.59	7.77	7.41	7.61	7.57	7.57	7.39	7.30

VITA

Miss Kitiya Lertskulbanlue was born on April 13, 1988 in Bangkok, Thailand. She graduated from Chulalongkorn University in 2010 and holds a Bachelor's degree of Science, major in Chemistry. After that she worked at Thaiparkerizing Co.,Ltd. as chemist during 2010-2011. Then, she has studied the Master's degree in Petrochemistry and Polymer Science Program, Chulalongkorn University, Bangkok, Thailand since 2011 and finished her study in 2014. During 2 years of study, she attended the oral presentation in the 26th International Symposium on Chemical Engineering that organized by The Society of Chemical Engineers, Busan, South Korea on 6-8 December, 2013 in the topic of "Preparation of ZSM-5/silica fiber by electrospinning for CO hydrogenation"